GROUND ELECTROMAGNETIC AND ELECTRICAL RESISTIVITY PROSPECTING FOR ORE MINERALISATION ZONES IN TSOHON-GURUSU NIGER STATE, NORTH-CENTRAL NIGERIA

BY

OGALE, Owoicho Daniel
MTech/SPS/2017/6962

DEPARTMENT OF PHYSICS, SCHOOL OF PHYSICAL AND APPLIED SCIENCES, FEDERAL UNIVERSITY OF TECHNOLOGY, MINNA

September, 2021

GROUND ELECTROMAGNETIC AND ELECTRICAL RESISTIVITY PROSPECTING FOR ORE MINERALISATION ZONES IN TSOHON-GURUSU NIGER STATE, NORTH-CENTRAL NIGERIA

BY

OGALE, Owoicho Daniel
MTech/SPS/2017/6962

A THESIS SUBMITTED TO THE POSTGRADUATE SCHOOL, FEDERAL UNIVERSITY OF TECHNOLOGY, MINNA, NIGERIA IN PARTIAL FULLFILMENT OF THE REQUIREMENTS FOR THE AWARD OF THE DEGREE OF MASTER OF TECHNOLOGY IN APPLIED GEOPHYSICS

September, 2021

ABSTRACT

To accurately explore and develop prospective mineral deposits, systematic geophysical approaches becomes a useful tool to establish areas of economically viable zones for exploration activities. This study integrates very low frequency electromagnetic (VLF-EM) and vertical electrical sounding (VES) methods of geophysical investigation to probe the subsurface in terms of its electrical conductivity characteristic to identify mineralised zones that could serve as possible host for conductive minerals and associated conductive metallic deposits in Tsohon Gurusu Area of Minna, North-Central Nigeria lying on latitude 9.621^{o}N to 9.625^{o}N and longitude 6.604^{o}E to 6.608^{o}E with an area extent of 250,000 m^{2}. A total of six profiles were investigated, each with length of 500 metres, 100 m inter-profile spacing and 20 m inter-station distance. The VLF-EM data were collected using Scintrex Envi VLF instrument. The acquired data sets were subjected to analysis and interpretation using MICROSOFT EXCEL, KHFFILT and OASIS MONTAJ software. Twelve points of significantly high and low conductivity were mapped out and sounded, adopting the Schlumberger array method with the help of ABEM Tarrameter SAS 4000 instrument and the data analysed using WinResist software. The result of the study indicated a general structural trend of NE-SW direction with significant conductivity responses due to inferred fracturing units containing conductive minerals as indicated by the peak responses of the current distributions and the surface and subsurface geologic features in the investigated profiles. Areas of high conductivity were observed in all the six profiles corresponding to fracture zones of interest as indicated in the current density sections, with profile 5 having the highest conductivity response of 135.5 mS/m and profile 6 with the least conductivity response of -136.7 mS/m. A general H-type curve were observed at VES 01, 02, 03, 04, 05, 06, 07, 10 and 12, VES 08 and 09 gave rise to an A-type curve indicative of majorly basement rock of granitic nature, however, VES 11 had a HK-type curve with five major layers with possible presence of conductive and non-conductive minerals. With reference to the obtained results from the study area, mineralisation is eminent and occurs within near surface fracture zones at estimated depth of 9 m.

TABLE OF CONTENTS

DEDICATION i

DECLARATION ii

CERTIFICATION iii

ACKNOWLEDGEMENTS iv

ABSTRACT v

TABLE OF CONTENTS vi

LIST OF TABLES viii

LIST OF FIGURES ix

LIST OF PLATES xi

ABBREVIATIONS, GLOSSARIES AND SYMBOLS xii

CHAPTER ONE 1

1.0 **INTRODUCTION** 1

1.1 Background to the Study 1

1.2 Statement of the Research Problem 2

1.3 Aim and Objectives of the Study 3

1.4 Justification of the Study 3

1.5 Scope of Work 4

1.6 Study Area 4

1.7 Geology of Nigeria 5

1.8 Geology of the Area 7

CHAPTER TWO 10

2.0 **LITERATURE REVIEW** 10

2.1 Introduction 10

2.2 Previous Related Geophysical and Geologic Literatures 11

CHAPTER THREE 18

3.0 **MATERIALS AND METHODS** 18

3.1 Introduction 18
3.2 Materials 18
3.3 Software 20
3.4 Methodology 20
3.4.1 Data collection 22
3.4.2 Field mapping 22
3.5 Electromagnetic surveying 22
3.5.1 Basic theory of electromagnetic surveying 23
3.5.2 Very low frequency electromagnetic survey (VLF E-M) 24
3.6 VLF Data Acquisition 27
3.6.1 VLF data filtering and analysis 27
3.7 Electrical Surveying 28
3.7.1 Resistivity surveying 29
3.7.2 Vertical electrical sounding 31
3.7.3 Refraction of current paths 31
3.7.4 Apparent resistivity 32
3.7.5 The Schlumberger array 32
3.8 VES Data acquisition 33
3.8.1 Data analysis 34

CHAPTER FOUR 35

4.0 **RESULTS AND DISCUSSION** 35
4.1 Results of Very Low Frequency Data 36
4.3 Vertical Electrical Sounding Data Analysis 47

CHAPTER FIVE 64

5.0 **CONCLUSION AND RECOMMENDATIONS** 64
5.1 Conclusion 64
5.2 Recommendations 65
5.3 REFERENCES 66

LIST OF TABLES

Table 3.1: Resistivity of some rocks and minerals 30

Table 4.1: Summary of sounding curves 63

LIST OF FIGURES

Figure 1.1: Map of Niger State, Nigeria, showing Tsohon Gurusu (GAMERS, 2018) 5

Figure 1.2: Geology of Nigeria. *Source*: Obaje, 2009 6

Figure 1.3: Geological map of the study area 7

Figure 1.4: Geological map of Niger State, Nigeria 9

Figure 3.1: Survey flow chart 21

Figure 3.2: Illustration of primary and secondary fields in the horizontal loop induction method of the electromagnetic exploration for shallow ore bodies 25

Figure 3.3: Resistivity survey graphic illustration 29

Figure 3.4: Current distribution 32

Figure 3.5: Schlumberger configuration 33

Figure 4.1: VLF1; unfiltered real (IP) and imaginary (Quad) 37

Figure 4.2: Profile 1; Fraser filter graph and 2D current density pseudo section 37

Figure 4.3: VLF2; unfiltered real (IP) and imaginary (Quad) 38

Figure 4.4: Profile 2; Fraser filter graph and 2D current density pseudo section 39

Figure 4.5: VLF3; unfiltered real (IP) and imaginary (Quad 40

Figure 4.6: Profile 3; Fraser filter graph and 2D current density pseudo section 40

Figure 4.7: VLF4; unfiltered real (IP) and imaginary (Quad) 41

Figure 4.8: Profile 4; Fraser filter graph and 2D current density pseudo section 42

Figure 4.9: VLF5; unfiltered real (IP) and imaginary (Quad) 43

Figure 4.10: Profile 5; Fraser filter graph and 2D current density pseudo section 43

Figure 4.11: VLF6; unfiltered real (IP) and imaginary (Quad) 44

Figure 4.12: Profile 6; Fraser filter graph and 2D current density pseudo section 45

Figure 4.13: Generalised conductivity map of the study area 46

Figure 4.14: Vertical Electrical Sounding 01 48

Figure 4.15: Vertical Electrical Sounding 02 49

Figure 4.16: Vertical Electrical Sounding 03 50

Figure 4.17: Vertical Electrical Sounding 04 51

Figure 4.18: Vertical Electrical Sounding 05 52

Figure 4.19: Vertical Electrical Sounding 06 53

Figure 4.20: Vertical Electrical Sounding 07 54

Figure 4.21: Vertical Electrical Sounding 08 55

Figure 4.22: Vertical Electrical Sounding 09 56

Figure 4.23: Vertical Electrical Sounding 10 57

Figure 4.24: Vertical Electrical Sounding 11 58

Figure 4.25: Vertical Electrical Sounding 12 59

Figure 4.26: Generalised VES resistivity map of layer 1 60

Figure 4.27: Generalised VES resistivity map of layer 2 61

Figure 4.28: Generalised VES resistivity map of layer 3 62

LIST OF PLATES

Plate I: Scintrex Envi VLF instrument 19

Plate II: ABEM SAS 4000 Terrameter 20

ABBREVIATIONS, GLOSSARIES AND SYMBOLS

VLF – Very low Frequency

EM – Electromagnetic

VES – Vertical Electrical Sounding

SAS – Standard Averaging System

NE – North East

SW – South West

mΩ - Milli-Ohms

mS/m – Milli-Siemens per meter

nT – Nano-Tesla

kHz – Kilo-Hertz

E – Electric field

B – Magnetic field

D – Electric field strength

H – Magnetic field strength

V/m^2 – Volts per meter square

C/m^2 – Coulombs per meter square

A/m – Amperes per meter

J – Current density

q – Charge

A_o – Original Frequency

Z_e – effective depth

μ_o - Magnetic permeability of free space = 4 $\times 10^{-7}$Henry/m.

ω - Angular frequency (2π)

σ - Electrical conductivity of earth material (mho/m)

ρ - Electrical resistivity

- Signal frequency.

CHAPTER ONE

1.0 INTRODUCTION

1.1 Background to the Study

Ores are metal/non-metal bearing minerals, or aggregates of metal-bearing minerals, more or less mixed with gangue. From the perspective on miners and/or metallurgists, they can be profitable (Evans, 2009). Among these metals are platinum, gold, silver, tin, copper, lead and zinc.

A country's ores and other mineral deposits constitute its natural wealth, which its development and prosperity is largely dependent on (Prasad, 2012); therefore, the degree of industrialisation of a country is directly related to the level utilisation of its mineral resources (Adekoya *et al*., 2011). Since the earliest, this recognition has led to mining and searching for metals (Telford *et al.*, 2001). Therefore, a large number of ore deposits are buried in the subsurface structure of the earth. Therefore, the systematic technology of exploring such ore bodies is essential to minimise the environmental degradation on the earth's surface (Oluwaseun, 2013).

Geological and geophysical surveys conducted by the Nigerian Geological Survey Agency and private exploration/mining companies continue to give people a better understanding of the country's mineral resources and potentials (Obaje, 2009), however, the environmental damages and hazards that accompanies the stages of mineral development such as the ecological adverse impact, alteration of natural flora and fauna, air, land, and water pollution, instability of lithostratigraphic masses, landscape devastation and radioactive exposures are neglected (Oluwaseun, 2013).

Exploration or Applied Geophysics tends to provide ecological friendly investigative methods to exploration, as well as the development of the Earth's confined resources through geophysical approaches by studying and enhancing the usage of such resources for human capital development. Geophysics suggests variety of methods of physical measurements of the Earth to carrying out systematic and scientific techniques for exploration of any sort. Hence, in mineral exploration, combination of two or more geophysical methods can be used to investigate and explore ore minerals irrespective of mode of occurrence, either massive or disseminated.

Geophysical methods of exploration, aims at detecting or inferring the presence of ore minerals, geothermic reservoirs, hydrocarbons, groundwater and other geologic structures employing surface methods to measure earth's physical properties and the their anomalies (Alisa, 1990).

Ground electromagnetic and electrical resistivity methods are parts of the main geophysical tools for investigating the subsurface for ores bodies (Kearey *et al.,* 2002). These methods detects subsurface zones with abnormal conductivity. Since these objects (different from ordinary rock forming metals, which are insulators) are characterised by considerable electrical conductivity, and their electrical conductivity ranges are different, this area of abnormally high electrical conductivity (or vice versa) is potential mineralised area of groundwater or conductive ore (Telford *et al.,* 2001).

1.2 Statement of the Research Problem

Nigeria's mining industry has been facing many challenges that have prevented growth from being achieved and limited the industry's potential and viability. Solving these key challenges will unlock the potential and prospect of the sector.

Due to the lack of policy and regulatory framework consistent with international best practices, and a lack of infrastructure to support the exploration and development of mineral resources, the apparent lack of systematically obtained detailed geo-scientific data has hindered the attraction of local and foreign investments to Nigeria's mining industry (Kullenberg, 2015), as such, this study addresses the need for the acquisition and application of geophysical data in prospecting for conductive minerals in Tsohon Gurusu area of Niger State, Nigeria using very low frequency ground electromagnetic and vertical electrical sounding methods.

1.3 Aim and Objectives of the Study

This research work is aimed at prospecting for subsurface conductive mineralisation zones using ground electromagnetic and electrical resistivity geophysical methods in Tsohon-Gurusu Area, Niger State, Nigeria. The objectives of the study are to;

i. produce surface geological map of the study area from geological reconnaissance survey;
ii. produce a generalised conductivity map of the area from the VLF data;
iii. determine the depth to top of conductive bodies from the vertical electrical sounding;
iv. produce resistivity subsurface layer maps from the vertical electrical sounding; and
v. delineate zones of possible conductive ore mineralisation.

1.4 Justification of the Study

This study area exhibits pathfinder rock materials which indicates potential mineral deposition, which is verified by features of mineralisation from the geology of the area, as well as the activities of artisan miners exploring for gold and other associated minerals in the area of study under consideration.

As such, with detailed geophysical survey data sets, exploration activities for minerals can be guided with precision, owing to the proper application of geophysical methods that indicate regions of mineralisation, and avoiding unnecessary environmental degradation activities due to wide-cat exploration.

Hence, local mining will be more successful when the geosciences data generated are utilised in directing trenching and pitting.

1.5 Scope of Work

This research was limited to the usage of Very Low Frequency Electromagnetic (VLF-EM) and the Vertical Electrical Sounding (VES) methods only on an aerial extent of 250,000 m^2, taking into cognizance the surface geology of the area.

1.6 Study Area

Location and Accessibility

Tsohon Gurusu lies along northeast of Bosso Local Government area of Niger State and the study area lies on latitude 9.621^{o}N to 9.625^{o}N and longitude 6.604^{o}E to 6.608^{o}E with an area extent of 250,000 m^2. The distance of the area from urbanised settlement is estimated to about 4.5 km from Maitumbi roundabout, Minna of which the site is about a km South-East, off Minna-Gwada road and it is spanned by a well accessible road either by foot or by vehicle.

The major activities in the study area includes; farming and artisanal mining, with farming predominantly taking a better part of the area where the land is arable, and consisting of patches of nomadic dwellers.

Figure 1.1 shows the map of Niger State, indicating Tsohon Gurusu which is the area of study lying along the eastern part of the state.

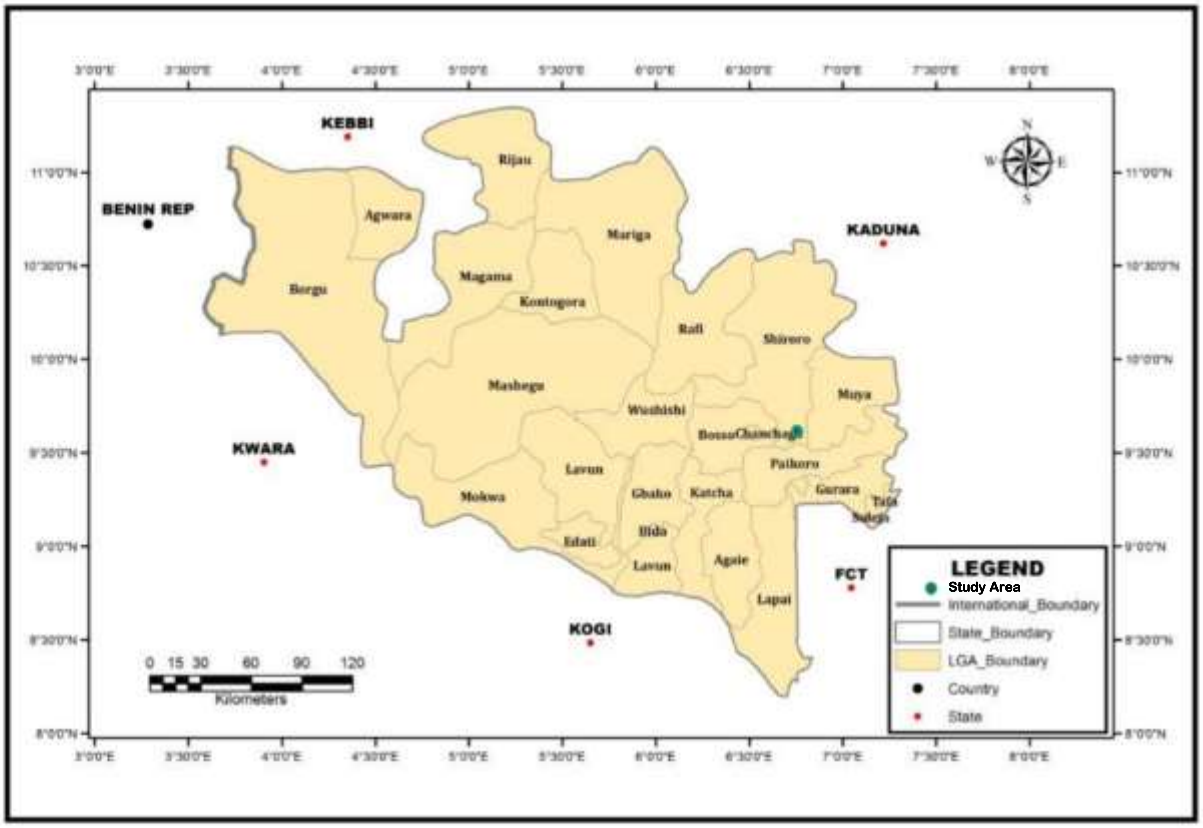

Figure 1.1: Map of Niger State, Nigeria, showing Tsohon Gurusu (GAMERS, 2018)

1.7 Geology of Nigeria

The geology of Nigeria consists majorly of three litho-petrological components, namely, the Basement Complex, Younger Granites, and Sedimentary Basins. The Basement Complex, which is Precambrian in age, is made up of the Migmatite-Gneiss Complex, the Schist Belts and the Older Granites (Obaje, 2009).

The Younger Granites is composed of several Jurassic magmatic ring complexes centered around Jos and other parts of north-central Nigeria. They are structurally and petrologically distinct from the Older Granites. The Sedimentary Basins, containing sediment fill of Cretaceous to Tertiary ages, comprise the Niger Delta, the Anambra Basin, the Lower, Middle and Upper Benue Trough, the Chad Basin, the Sokoto Basin, the Mid-Niger (Bida-Nupe) Basin and the Dahomey Basin.

Mineral deposits are economically available in all the components of Nigerian geology. Solid gmineral deposits of economic significance that include gold, iron ore, cassiterite, columbite, wolframite, pyrochlore, monazite, marble, coal, limestone, clays, barites, lead-zinc, etc, occur in the different geologic segments of Nigeria (Obaje, 2009).

Figure 1.2 shows the general geology of Nigeria, comprising the distribution of the major geological formations in each region, with the area under investigation lying within the basement complex in the North-Central region of Nigeria.

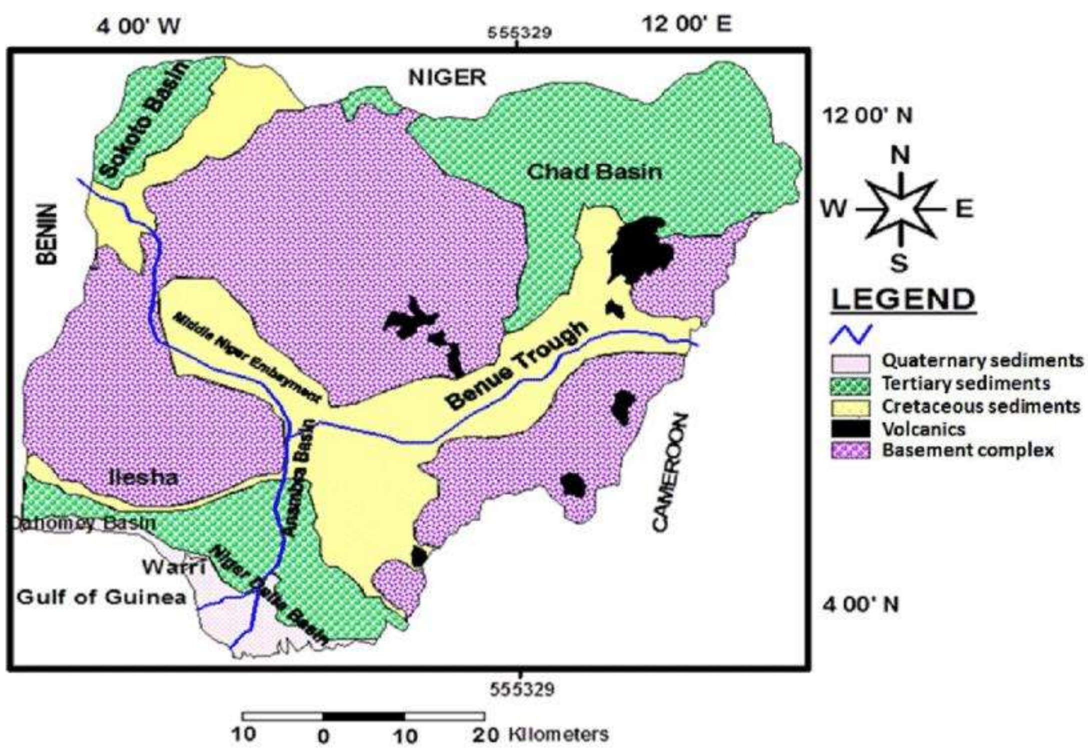

Figure 1.2: Geology of Nigeria. *Source*: Obaje, 2009

1.8 Geology of the Area

The study area is located in the basement complex of Nigeria. It is one of the three main litho-petrological components of Nigerian geology (Obaje, 2009). It is part of the Pan-African moving belt, located in West African and Congo Cratons and Taureg Shield (Taureg Shield) south (Black, 1980). It is invaded by the Mesozoic calc-alkaline ring complex (younger granite) of the plateau, and is unconformably covered by Cretaceous and younger sediments (Obaje, 2009).

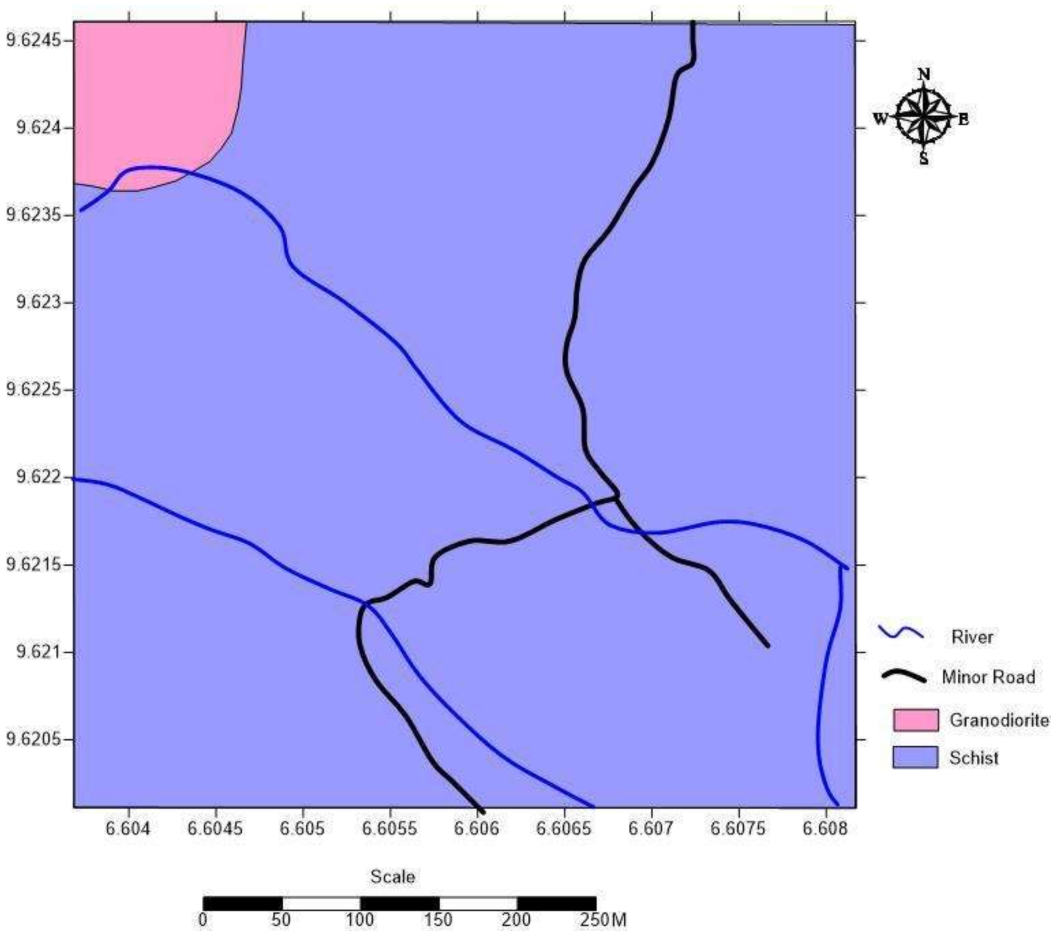

Figure 1.3: Geological map of the study area

Figure 1.3 shows the localised geological map of the study area, chiefly consisting of schist, patches of outcropping metamorphic rocks and major stream channels.

The basement complex is divided into the Western and Eastern provinces. The Western province is located west of longitude 8^0 E, represented by N-S, centered on the NNE-SSW trend schist belts, these schist belts are separated from each other by migmatites, gneisses and granites. It is believed that the trend is the result of Pan-African orogenic movement, involving collisions between the West African Craton and Pan-African active terrain and eastward subduction zone (Ajibade *et al.,* 1979). The schist belts are differently interpreted as small ocean basins (Ajibade *et al.*, 1989), in filled rift structures (Ball, 1980) or synclinal remnants of an extensive supra-crustal cover (Barley and Wright, 1989).

The basement complex in Nigeria consists of four main rock lithology units namely;

1. The Migmatite – Gneiss Complex (MGC)
2. The Schist Belt (Metasedimentary and Metavolcanic rocks)
3. The Older Granites (Pan African granitoids)
4. Undeformed Acid and Basic Dykes

The schist belt consist of approximately N-S trending narrow zones of low medium grade metamorphic rocks of mainly sedimentary and minor igneous origin which were deposited previously on the pre-existing gnesiss-magmatite-quartzite basement (Adekoya *et al*., 2011). The area lies on the Kushaka schist belt, which distinguishes itself forming a number of curving schist belts, differentiated by domes and anticlines of gneiss (Obaje, 2009). The major type of rock is semi-pelitic biotite-muscovite schist, located within areas containing garnet and staurolite. Others are metasiltstones, phyllites and graphitic schists. Several dense units of banded garnetgrunerite iron formation are interbedded with the schists. Varying amphibolites and amphibole, epidote, chlorite and talc-bearing schists conforming to a least partly to tholeiitic basalt (Elueze, 1981). The Kushaka schist belts are intruded largely by plutons of granodiorite, granite and syenite, which often interfuse into the axial zone of the belts (Obaje, 2009).

Figure 1.3 shows the generalised geological map of Niger State, indicating Tsohon Gurusu which lies with the basement complex of the state.

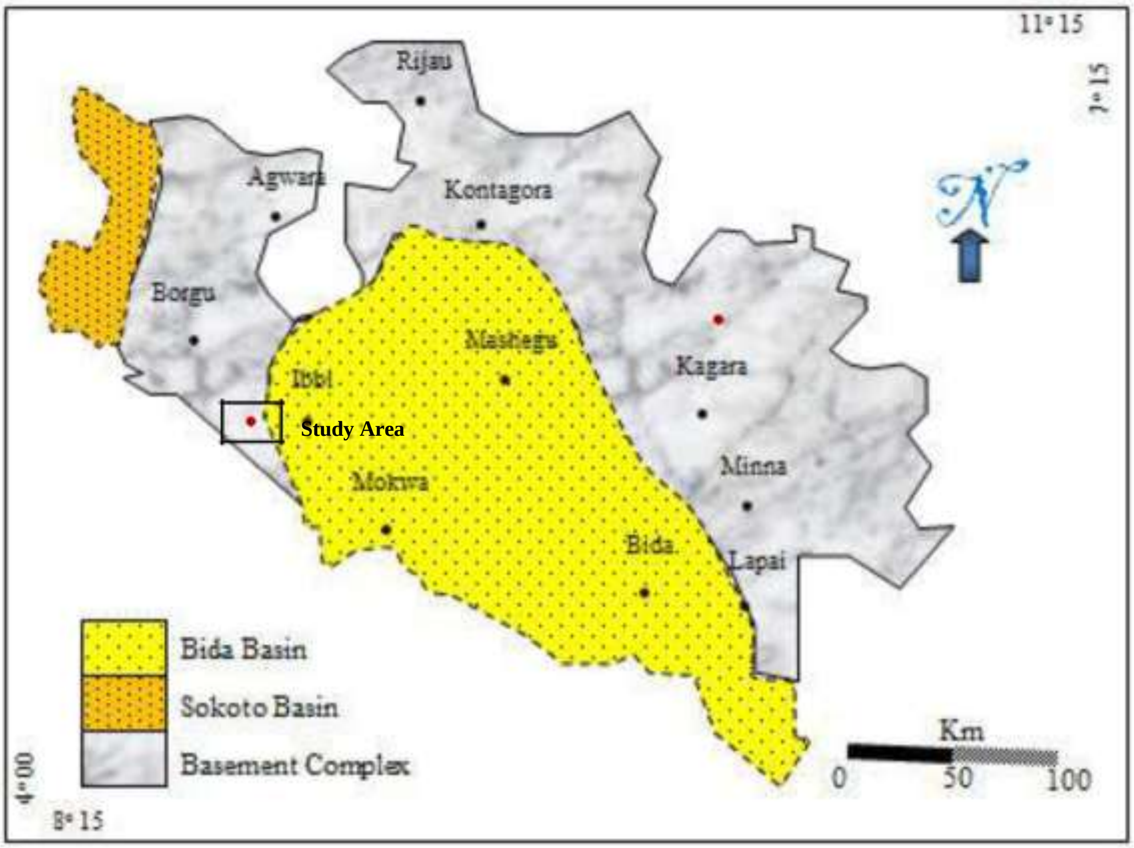

Figure 1.4: Geological map of Niger State, Nigeria

CHAPTER TWO

2.0 LITERATURE REVIEW

2.1 Introduction

The review of past literatures in relevance to this work are correlated with numerous ways and findings to either improve on them or develop new theories for the effective location and development of economically viable conductive ore bodies deposited on the surface and within the subsurface.

Conducting any geophysical survey demands the geoscientist to meticulously choose amongst the geophysical methods applicable to locating target of interest which is able to yield the most effective distinction in identifying the target from different sources of anomalous characters, hence, in conductive ore bodies delineation, handful numbers of applicable geophysical methods are often employed to investigation these contributory bodies of anomalous characteristics within the subsurface, such methods would include electrical and electromagnetic methods (Richard *et al*., 2013)

Structural characterization of the subsurface for ore mineralisation delineation involves integration of geologic findings and geophysical investigations and their corresponding interpretations to distinctively isolate these bodies from other intrusive bodies with pseudo responses. This work was centred on the applicability of electrical and electromagnetic methods in establishing the characteristic options well-known for the indication of conduction zones to find these conductive bodies. As such, previous literatures involving prospecting and delineations of mineralised zone were reviewed with regard to the geophysical methods utilized and their corresponding findings.

2.2 Previous Related Geophysical and Geologic Literatures

Subsurface geophysical investigations are practical proceeding and high resolution results demand specific geophysical methodology in a focus to delineating anomalies (McGaughey *et al*., 1997), rendering the likelihood of integrating many geophysical approaches to ore mineral exploration and appraisal.

Shehu *et al*. (2019) carried out a reconnaissance study to delineate the potential mineral zones around the schist belt areas of Kano State, Nigeria using airborne magnetic data and their results indicated that, anomalies with short wavelength recorded within the area of study, of range -99.182 to 88.338 nT show the area to be characterised by crystalline basement complex structures. And results of the vertical derivatives indicates that lineaments that delineate veins of possible mineralisation exist within the area. The lineaments trends in the NE-SW and E-W directions with the NE-SW being dominant. Their assertion pertaining structural trends in the study area coincides with the general trends of the basement complex of the Northern a part of Nigeria and verifies the geologic structural trends of rock structures on a regional scale, also validates the reconnaissance survey carried out to investigate the structural trend exhibited by the structures in the area of study.

Integration of Aeromagnetic Interpretation and induced Polarisation methods in Delineating Mineral Deposits and Basement Configuration within Southern Bida Basin, North-West Nigeria was carried out by Usman *et al.* (2019) and through the analysis of the induced polarisation data, the potential mineralisation fracture area is depicted from the pseudo-section of the resistivity and chargeability contour map. The qualitative interpretation results of each resistivity and chargeability pseudo-section show the potential fracture area in the eat-west direction (E-W) trend, and the depth range from the anomaly body is (0.3 to 2.5

km), and the average overburden thickness is 2.1 km. The typical resistivity and chargeability values ranges from (5.17 to 42.4Ωm) and (1.10 to 42.3ms) respectively. They concluded that based on the calculated deposition thickness, geothermic gradient and current fractures, the possibility of hydrocarbon accumulation in the north and southeast of the area is feasible, while other parts of the area with low deposition thickness maybe susceptible to magnetic mineral. Suggesting that mineralisation preponderantly occur in basement complexes, justifying the need to employ other geophysical investigate measures in delineating conductive zones .

Analysis of aeromagnetic anomalies and structural lineaments for mineral and hydrocarbon exploration in Ikom and its environs Southeastern Nigeria was carried out by Arinze *et al*. (2018) where the aeromagnetic data were enhanced by the transformation of the regional-residual analysis to get the deeper magnetic sources. They obtained two depth sources using the well-known Peters half-slope technique. The deeper anomaly source depth is approximately 0.83 km–3.5 km of field intensity range of −30 nT to −220 nT whereas the skin-deep sources ranges between 0.2 km–0.75 km with magnetic intensity varying from −10 nT to 20 nT, and these are as a result of the underlying Precambrian basement formations and intra basement structures conforming to fractures and faults however, the skin-deep sources are because of basement intrusions as well as veins containing ores confined within the superimposed Cretaceous rocks. The superficial basement depth and presence of intrusions and linear structures indicates that the area possibly exhibit good mineral prospects however unfavourable for hydrocarbon formation. Hence, the work suggested that mineralisation occur among intrusions and structural veins.

Akinlalu *et al*. (2018) employed aeromagnetic method to map basement structures and characterization of zones of mineralisation in Ilesa Schist Belt, Southwestern Nigeria by estimating the depth to the deep, intermediate and near surface structures based on the Spectral analysis and Euler deconvolution of the aeromagnetic data and correlated the results with the geology of the area, they extracted the magnetic anomalies from the RTE map with amplitude range of -115 to 134 nT, showing high magnetic intensities occurring over amphibolite, schist, porphyritic granite, gneiss and undifferentiated Migmatite, and low intensities were recorded over quartzite and the undifferentiated schist. Hence, concluded that the depicted structures were assumed to host minerals and as observed from artisanal mining within in the area.

Ejepu *et al*. (2018) employed Geological, Multispectral and Aeromagnetic Expressions of Pegmatite Hosted Mineralisation of Keffi Sheet 208 NE, North-Central Nigeria, to characterise specific spectral and geophysical features in an attempt to narrow down areas for further mineral exploration. Inferences were drawn that pegmatite bodies are more prominent in the schist, geologic boundaries and contact zones and a few shear zones have metal bearing pegmatites whereas, foliation planes (schist and gneiss) and fractures of granites are all wealthy with pegmatite veins and dykes. Rare-metal pegmatites are near to major and subsidiary fault structures. They hence, concluded that the combination of remote sensing data with information from the aeromagnetic data led to the identification of probable locations pegmatite hosted mineral occurrences.

Osinowo and Falufosi (2018), used integrated ground magnetic and very low frequency electromagnetic (VLF-EM) methods of geophysical investigation to examine the subsurface in terms of rock magnetic susceptibility and ground conductivity for the aim of identifying pegmatite vein mineralisation that may serve as host for gold and other associated metallic deposits and delineate mineralised pegmatite vein around Ihale in Bunnu-Kabba area of Kogi, north-central Nigeria. They obtained seven relatively high VLF-EM regions from the current density, and the matched high residual positive magnetic anomaly showed characteristics closely realted to the underground response obtained near the determined profile. The local mineral deposit activity indicated that the gold mining and the pegmatite veins in this section were established on the basis of evidence mineralization.

Dogara and Alao (2017) carried out Preliminary Estimate of Gypsum Deposit Based on Wenner and Schlumberger Electrical Resistivity Methods Ikpeshi, Edo State, Nigeria. Formation common to the area of study was identified to be limestone, having varying range of resistivity values (1 – 104 Ω-m). The investigated area showed the traces/crystals of gypsum at depths ranging between 3 m and 9 m, with 1 to 3000 Ω-m resistivity range spread around the area. The estimated gypsum reserve is about seventeen million tons. The survey indicated that gypsum crystals is possibly associated with the major limestone/clay/shale formation in the area of study.

Sriramulu *et al*. (2017) in their work demonstrated the application of Very Low Frequency Electromagnetic, Magnetic and Radiometric Surveys for Lamporites Investigation in Vattikod Area of Nalgene District, Telangina State, India, characterizing the effectiveness of the very low frequency method to map subsurface variations of geological structures, faults/fractures disposition, dyke extent and contact between various rock present in the area of study and were able to obtain distinctive results of the VLF analysed data from the Fraser and Karous-Hjelt filter generating the 2D inversion current density pseudo sections for the real and imaginary components, which helped the delineation and refining of the location of the conductors which are primary indicators of Lamporites deposit in the survey area.

Olawuyi *et al*. (2016), in their work titled Aeromagnetic Data and Pseudo-gravity Transforms in Mineral Exploration: A Case Study of Pegmatite Rich Zones of Lafiagi, Central Nigeria applied the 3D Euler deconvolution on the aeromagnetic data to delineate the spatial distributions of the mineralised zones in the area and revealed that structures associated with pegmatite are rich in minerals, inferring that pegmatites structures can give rise to anomalous responses when geophysical investigations are carried out on host rocks, however, anomalies observed by geophysical investigation methods are based on specific mineral of interest as such, are characteristic to target minerals.

Onwuegbulam *et al*. (2016), investigated fractures and conductive zones in Auchi, south-western, Nigeria, obtaining sparsely fractured zones of low conductivity indicating massive resistive rock. The VLF method which is very much applicable in groundwater, minerals prospecting and engineering works like road construction, to indicate/locate weak and consolidated zones of faults/fractures, these fractured zones are considered to host or feature subsurface water ways and point of interest in mineral deposition.

Akintayo *et al*. (2014) used magnetic and resistivity geophysical methods to investigate the location and depth of mineral rocks at Olode village, Oyo State, Nigeria by evaluating areas of high magnetic intensities with corresponding low resistivities (high conductivities), as areas of possible mineralisation, with reference to the geological setup of the study area. Findings from the work tend to relate structures with high magnetic intensities with corresponding high conductivity as zones of possible mineralisation. However, not all mineral are magnetic and conductive as such none magnetic and low conductive mineral may exist in the area. Therefore, choice of investigative method can be made target specific. Austin *et al*. (2014) carried out an Evaluation of Self-Potential Anomalies over Sulphide Ore Deposits at Ishiagu, Ebonyi State, Southeastern Nigeria. Their results indicate a positive self-potential effect, and there are corresponding peaks in the profile, indicating that there are sulphide depositsthe trend dirention of the anomaly peak appears roughly in NW-SE and the transverse stress mode (NE-SW). Therefore, it can be concluded that in the anomaly change in SP, the best diagnosis is a positive SP because it indicates the presence of sulphide ore The result indicates that peaks shown/observed in any geophysical investigation is of interest in locating whatsoever target is in question, since they are indicative of anomalous responses.

Ogungbemi *et al*. (2014) undertook a research involving the Integrated Geophysical Approach to Solid Mineral Exploration: A Case Study of Kusa Mountain, Ijero Ekiti, Southwestern Nigeria. The very low frequency electromagnetic (VLF-EM) profile was measured along the eight lines and conductive (fractured) area was established. In this way, 10 vertical electrical sounding (VES) points can be located on the obvious fault zone and further analysed to reveal the mineralised zone. The constraint model developed with reference to the results of VLF-EM and resistivity supports the W-E trend mineralization zone in the central and northern regions. VLF-EM results show that fractures (positive anomalies) are suspected to be the migration path of depicted mineral characterised with zones of positive and negative anomalies of VLF-EM responses ranging from -9.9% to 7.0%. This research which combined VLF-EM and geo-electric methods revealed potential and trends of mineral occurrence in the W-E, structurally controlled and highly localized in the Kusa mountain, Ijero Ekiti.

Tijani *et al*. (2009) in their work, mapping of sub-surface fracture systems using integrated electrical resistivity profiling and VLF-EM methods: a case study of suspected gold mineralisation, located at the outskirt of New-Bussa, Niger State, Nigeria. They used Horizontal Resistivity Profiling and the Very Low Frequency data to qualitatively interprete and reveal many subsurface areas with high real component current density, these areas define potential subsurface structural features (such as fault zones) for possible gold mineralization. Correlation and extrapolation of abnormally low resistivity regions and high current density regions reveals that fracture system, which is interpreted as potential or inferred structurally controlled fracture regions, are possible gold mineralization zones.

Ezeh *et al*. (2004), Evaluated the very low frequency electromagnetic (VLF-EM) response of the lead sulphide deposit in the Abakaliki lead/zinc mine in Nigeria to study the lateral extension of the mine and determined tool's simplicity in mapping the potential of the sulphide deposit in the underlying area. Inexpensive tools have successfully mapped a deposit of about 40 m long composed mainly of shale and strikes NW–SE following one of the major faults. The conductor were estimated to be 10 m of depth and dipping at 90°. Hence, inferring that dip angles of conductive bodies can also be obtained from VLF data to delineate structural orientation of conductive bodies.

CHAPTER THREE

3.0 MATERIALS AND METHODS

3.1 Introduction

Conducting any geophysical survey requires the deployment of multiple skills, putting into cognizance the appropriate manpower, tools, geophysical methods, equipment and materials to obtaining quality data which should reflect the true picture of the anomaly under investigation.

3.2 Materials

1. Garmin etrex10 Global Positioning System (GPS)
2. Compass clinometer
3. Measuring tapes
4. Current and potential electrodes
5. Hammer
6. 24 Volt Battery
7. Cables and rails
8. Data sheet
9. Pegs
10. Ribbons
11. Scintrex Envi VLF instrument
12. ABEM SAS 4000 Tarrameter

Plate I, displays image of the VLF-EM equipment deployed for the acquisition of the VLF data.

Plate I: Scintrex Envi VLF instrument

Plate II, displays ABEM Terrameter SAS 4000 deployed for acquiring the VES data.

Plate II: ABEM SAS 4000 Terrameter

3.3 Software

1. Microsoft Excel 2010
2. Karous-Hjelt
3. Oasis Montaj 6.4.2
4. WinResist

3.4 Methodology

Figure 3.1, illustrates the graphical representation of steps in sequential order on how the survey plan was deployed and executed for the investigation.

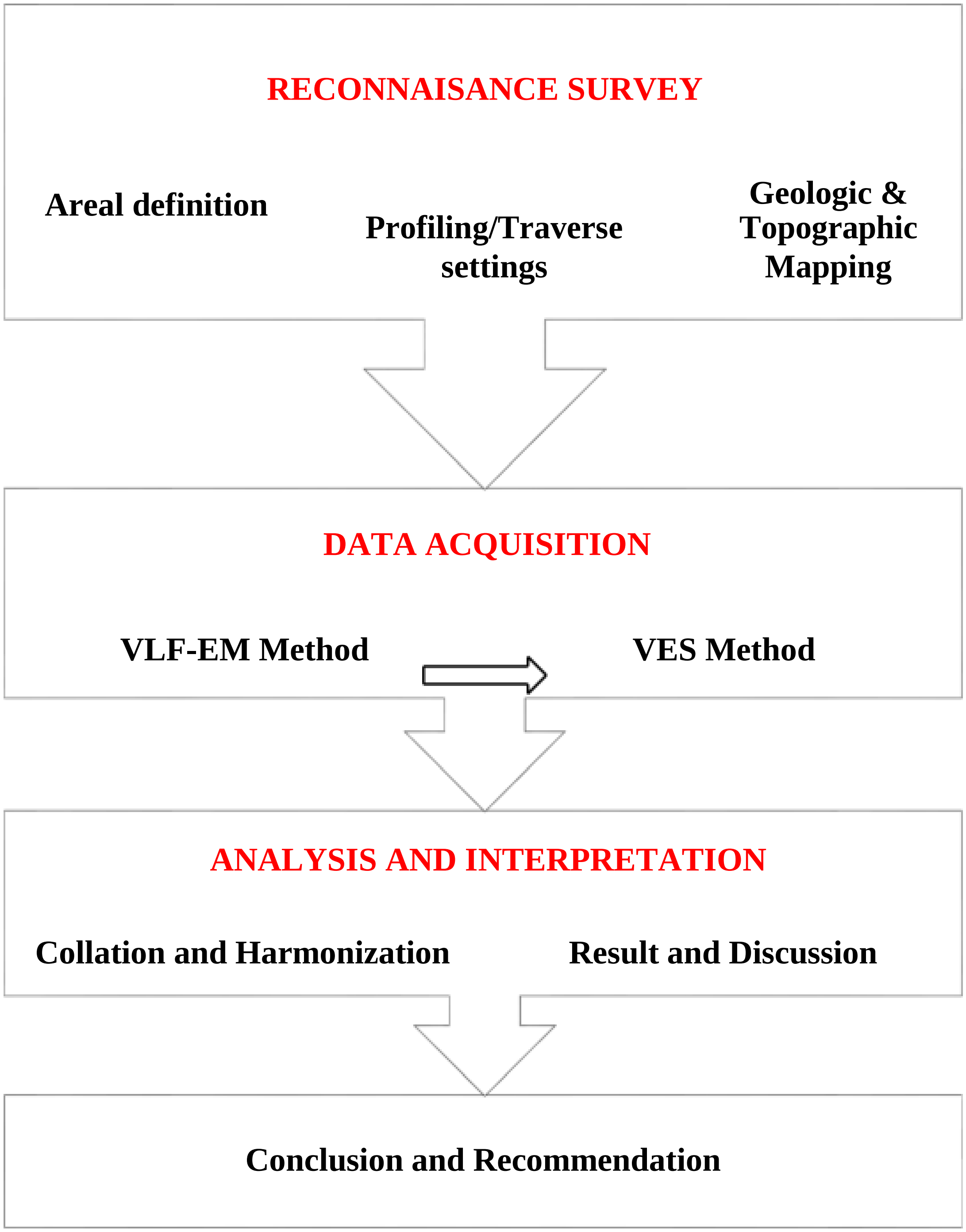

Figure 3.1: Survey flow chart

3.4.1 Data collection

In this section, details of how field data were acquired by the deployment of the GPS, VLF instrument and the Resistivity meter is discussed in relation to all the procedures employed to generating high quality data that represents the true surface and subsurface features.

3.4.2 Field mapping

Areal expanse was established by defining boundaries for investigation using a GPS and geological reconnaissance of the delineated work area was conducted to determine the regional strike of the rock foliations. Geologic mapping was also carried out to generate the map indicating the different outcrops of rocks in the area.

3.5 Electromagnetic surveying

Electromagnetic surveys investigated at frequency lower than 50 kHz are influenced the electromagnetic principle of induction. The alternating magnetic field in the coil or cable induces current in the conductor, and then measures the earth's conductivity (σ in Siemens/m) (Scott, 2014). The conductivity of rock and soil is too poor to produce a large induced current, but if there is a good conductor, an eddy current system will be established. In this way, the secondary magnetic field generated by the eddy current is superimposed on the primary magnetic field and can be measured on the surface (Telford *et al.,* 2001).

This principle is used to evaluate subsurface electrical conductivity (Telford *et al.,* 2001). Ground contact is not required hence, neglects direct coupling problem. This enables quick data collection (Gordon, 2016). Consequently, it is often used as reconnaissance tool to delineate anomalies for more detailing.

Electrical and electromagnetic methods have been deployed successfully to detect and delineate conductive ore bodies both on surface and in the subsurface, (Mwenifumbo, 1997).

3.5.1 Basic theory of electromagnetic surveying

In electromagnetic (EM) surveys, the electrical conductivity of the ground is measured based on depth and/or horizontal distance. Different rocks (and buried structures/objects) produce different conductivity values. Plotting changes in conductivity can indicate anomalous areas worthy of further geophysical or intrusive investigation.

The electromagnetic method is based on the magnetic components of electromagnetic waves generated on the ground to induce current in the subsurface. Alternating current with varying frequency passes through the coil (transmitting coil). This process generates an alternating primary magnetic field, and then induces very small eddy currents in the subsurface. The size of the eddy current is proportional to the conductivity of the surface near the coil. These eddy currents then generate a secondary magnetic field, part of which is captured by the receiving coil. The interaction between the primary and secondary magnetic flux and the receiver coil creates a voltage related to the conductivity of the subsurface in milliSiemen/metre (mS/m) (Lowrie, 2007).

This electromagnetic field may be defined in terms of vector function ***E***, ***D***, ***H***and ***B***, where:

i. ***E*** is the electrical field in V/m^2

ii. ***D*** is the dielectric displacement in C/m^2

iii. ***H*** is the magnetic field intensity in A/m

iv. ***B*** is the magnetic induction in Tesla

$$= - \quad — \tag{3.1}$$

Faraday’s law (Electrical field generated by magnetic field with varying time)

$$= + \quad — \tag{3.2}$$

Ampere’s law (Magnetic field generated by a time varying electric field)

Maxwell’s equations

$$= \tag{3.3}$$

The magnetic induction line is continuous, there is no single magnetic pole

$$= \tag{3.4}$$

Electrical fields can begin and end on electrical charges

3.5.2 Very low frequency electromagnetic survey (VLF E-M)

The VLF-EM method is an active method which uses frequencies generated by transmitters in the far field. These signal frequencies are generated by very powerful radio transmitters from Military bases in the United States of America and from other countries for the aim of communication with their submarines (Scott, 2014) and they are mostly within the ranges of 15-30 kHz, transmitted for hundreds or thousands of kilometers, the curvature of the wave fronts is so almost negligible that they are effectively flat (Alan *et al.,* 2000).

Figure 3.2, shows that the transmitted electromagnetic wave propagates above or near the surface of the earth. The induced magnetic field generated by the displacement current is shown by the primary magnetic field, and the phase shift occurs when it encounters the conductor. Therefore, the conductor becomes the source of another field (secondary). As such, electrical characteristics of the subsurface can be obtained by comparing the primary and secondary field.

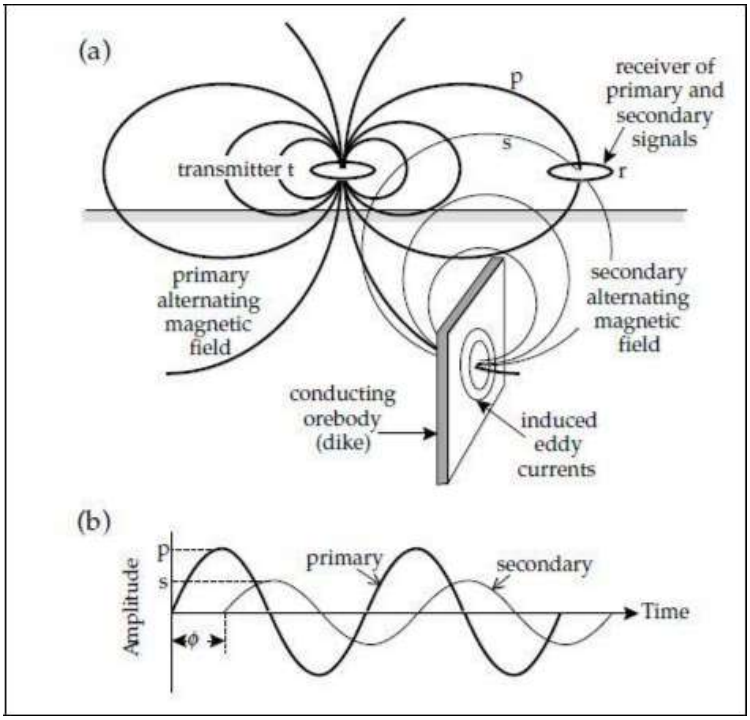

Figure 3.2: (**a)** The illustration of primary and secondary fields in the horizontal loop induction method of the electromagnetic exploration for shallow ore bodies. **(b)** The amplitude and phase of the main (p) and secondary (s) fields *(Lowrie, 2007).*

The penetration depth of the transmitted electromagnetic waves depends on their frequencies and the electrical conductivity of the subsurface. This depth increases as both the frequencies and subsurface conductivity decreases (Kearey *et al.*, 1984).

$$= \sqrt{\frac{2}{\;}} \cong \frac{500}{\;} = 500\sqrt{\frac{\;}{\;}} \qquad (3.5)$$

δ = Skin depth in meters (Depth of penetration of e-m wave passing into a conductor in which the amplitude of the wave is attenuated to 1 of its amplitude at the surface of the conductor).
μ_o = Magnetic permeability of free space = 4 $\times 10^{-7}$Henry/m.

ω= Angular frequency (2π)

σ = Electrical conductivity of earth material (mho/m)

ρ = Electrical resistivity

= Signal frequency.

The amplitude of electromagnetic fields decreases exponentially with depth. The amplitude of EM radiation is a function of depth relative to its original amplitude, A_o, and is given by

(3.6)

At great distances from the source of electromagnetic waves, this type of attenuation will control the depth of investigation. The effective investigation depth , defines the maximum depth at which the body can be buried and still produces an identifiable signal higher than noise. It is given by Kearey *et al*. (1984) as

$$= 100\sqrt{} \quad (3.7)$$

The VLF instrument detects the primary and secondary fields, and divides the secondary field into in-phase and quadrature components according to the phase lag of the secondary field. These components of the secondary field can also be referred to as tilt (in-phase) and ellipticity (quadrature) (Pirttijärvi, 2004). When the VLF-EM method is used in geophysical surveys, the in-phase response is sensitive to metals or good electrical conductors (Lazarus *et al.*, 2013). On the other hand, the quadrature response is very sensitive to changes in the electrical characteristics of the earth (Jeng *et al*., 2004).

$$= h = \tan(\ ) * 100\% \qquad * 100\% \quad (3.8)$$

$$= \quad (3.9)$$

3.6 VLF Data Acquisition

The areal expanse was established by defining boundaries for investigation using a Global Positioning System (GPS). Geological reconnaissance of the delineated work area was conducted to determine the regional strike of the rock foliations. Geologic mapping was also carried out to generate the map indicating the different outcrops of rocks in the area.

A total of six (6) survey profil es with East-West orientations which is perpendicular to the strike foliation, having inter-profile distances of 100 m and inter-station spacing of 20 m along each profile were generated across the strike formations, hence a total of 156 VLF stations were established, and from which VLF data was generated from each point of interest.

The Scintrex Envi VLF Instrument was deployed in this investigation and oriented along the frequency transmitter, and a frequency of 21.1 kHz signal with call-sign RDL from Russia having the best signal strength was selected.

Plate III, shows VLF data being collected at the established stations which are along the dip direction (along profiles) of the rock outcrops in order to reveal the lithologic variations, (because lithologic variations occur along the dip direction and the dip direction is perpendicular to the strike).

3.6.1 VLF data filtering and analysis

In order to overcome the influence of time changes in the magnetic field (for example, due to changes in the waves guided by the surface and bottom of the ionosphere), Fraser (1969) designed a simple numerical filter (Fraser filter) to convert the cross-over to continuous in-phase components. The value is differentiated by 90^{o} along the direction of the curve to distinguish the continuous value of the in-phase component, thereby converting the current polarity to the peak value. The VLF data was then subjected to analysis on MICROSOFT EXCEL and qualitatively interpreted using OASIS MONTAJ software.

3.7 Electrical Surveying

Thee important physical properties of rocks used for electrical measurement are the permittivity (for georadar) and resistivity (or conductivity), which are the basis of several methods. Anomalies occur when conductors (such as mineralized dykes or ore bodies) are present in rocks with high resistivity of different rocks and minerals vary greatly, the resistivity difference between the ore body and the main rock is usually very large. For metal ore minerals, the resistivity may be low, but the igneous rock that does not contain water may have a high resistivity, and the presence of groundwater will also affect the resistivity of the rock that acts as an electrolyte. Therefore, it occurs in porous sediments and sedimentary rocks.

The minerals that form the rock matrix are generally inferior to the conductor of groundwater, so the conductivity of the sediment increases with the amount of groundwater contained in it. The conductivity of the rock is directly proportional to the conductivity of the groundwater, which is very variable because it depends on the concentration and type of minerals and salts.

The observation of these phenomenal quantities can be expressed by the formula for resistivity of rock called Archie's law:

$$= \frac{\quad}{\emptyset} \tag{3.10}$$

Given by, ϕ and *S* are fractions between 0 and 1, is groundwater resistivity, and *a*, *m* and *n* are empirical constants. Typically, $0.5 \leq \leq 2.5$, $1.3 \leq \leq 2.5$ and $n \approx 2$ (Lowrie, 2007).

3.7.1 Resistivity surveying

Resistivity surveys use wires connected to the ground to investigate the horizontal and vertical changes in the subsurface resistance (or conductivity, the reciprocal of resistivity) by passing current through the ground. As shown in Figure 3.3 the process is to measure the potential on other electrodes near the current, from which the apparent resistivity can be measured. (Telford *et al.*, 2001).

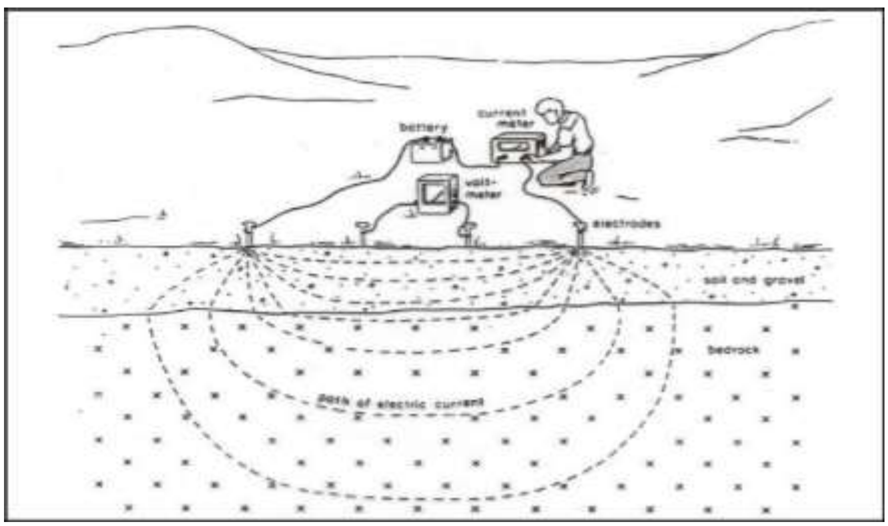

Figure 3.3: Resistivity surveying graphic illustration (Marescot, 2004)

Table 3.1, constitute some rocks and minerals with their corresponding approximate resistivity values. Igneous rocks have the highest electrical resistivity, while sedimentary rocks tend to have the greatest electrical conductivity due to their higher fluid content. Metamorphic rocks have moderate but overlapping resistivities. (Reynolds, 2011).

Table 3.1: Resistivity of some rocks and minerals (Alan *et al.*, 2000)

Rocks, minerals, ores	Resistivity (ohm-m)
Sediments	
Chalk	50-150*
Clay	1-100
Gravel	100-5000
Limestone	$50\text{-}10^{7}$
Marl	1-100
Quartzite	$10\text{-}10^{8}$
Shale	10-1000
Sand	500-5000
Sandstone	$1\text{-}10^{8}$
Igneous and metamorphic rocks	
Basalt	$10\text{-}10^{7}$
Gabbro	$1000\text{-}10^{6}$
Granite	$100\text{-}10^{6}$
Marble	$100\text{-}10^{8}$
Schist	$10\text{-}10^{4}$
Slate	$100\text{-}10^{7}$
Minerals and ores	
Silver	1.6×10^{-8}
Graphite, massive ore	$10^{-4}\text{-}10^{-3}$
Galena (PbS)	$10^{-3}\text{-}10^{2}$
Magnetite ore	$1\text{-}10^{5}$
Sphalerite (ZnS)	$10^{3}\text{-}10^{6}$
Pyrite	1 x100
Chalcopyrite	1×10^{-5} - 0.3
Quartz	10^{10} - 2×10^{14}
Rock salt	$10 - 10^{13}$
Waters and effect of water and salt content	
Pure water	1×10^{6}
Natural waters	$1\text{-}10^{3}$
Sea water	0.2
20% salt	5×10^{-2}
Granite, 0% water	10^{10}
Granite, 0.19% water	1×10^{6}

3.7.2 Vertical electrical sounding

Vertical electrical sounding (VES) also called depth sounding or sometimes an electric drill is used when the subsurface similar to a series of horizontal layers, each of which has a uniform but different resistivity. The essence of VES is to expand the electrode array from a fixed center, though some current spreads down into all layers, nearly all was in the top layer, so the resistivities of lower layers have negligible effect on the current paths or on the readings. This is no longer true when the separation has been expanded to be comparable to, or larger than, the depth to the second layer and then the presence of the second layer was detected.

The vertical electrical sounding (VES) is very popular in conventional geophysical studies, such as in environmental investigations, oil and gas exploration, coal and other metallic ore prospecting (Keller *et al*., 1966).

3.7.3 Refraction of current paths

Figure 3.4, In uniform layer, the current paths are smooth curves, but when they pass through the interface separating different resistivities, they bend or refract. When entering the rock with higher resistivity, they will refract to the normal; conversely, when entering the rock with lower resistivity, they will refract to the normal. Since refraction changes the distribution of current in the layered subsurface, the ratio $\Delta V/I$ also changes compared to uniform grounding, which makes it possible to measure the change in resistivity with depth.

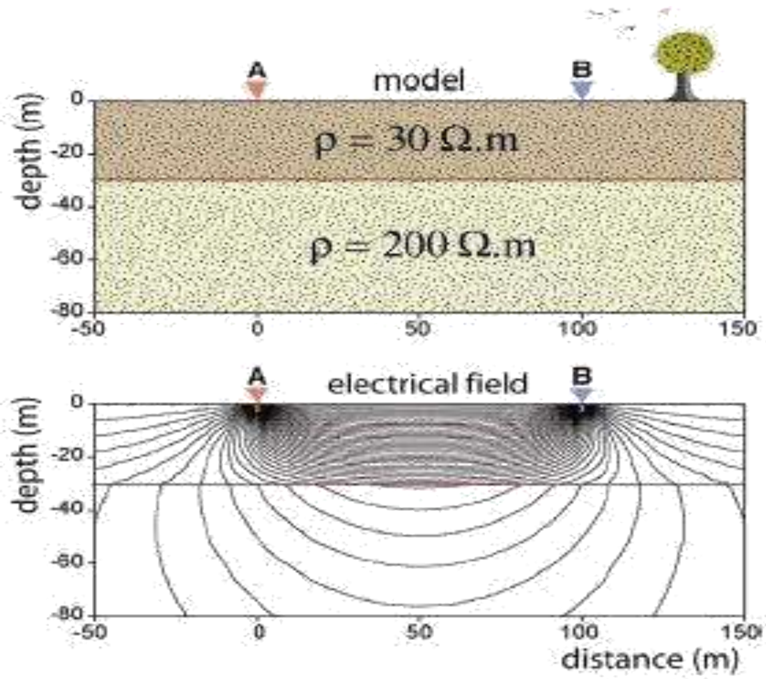

Figure 3.4: Current distribution (Marescot, 2004)

3.7.4 Apparent resistivity

In a VES survey, the ratio of current to p.d., Δ / , the measurement is taken with increasing electrode spacing. There are two reasons for the changes in this ratio, because the resistivity changes with depth and the electrodes are being moved apart. This second effect has to be allowed for before the first the object of the survey can be deduced.

$$= \quad (3.11)$$

= Apparent resistivity

Δ = potential difference

= Current

= Geometric factor (dependent on array configuration

3.7.5 The Schlumberger array

The Schlumberger array places potential (P) electrodes symmetrically about the centre of the array. Readings are taken with only the current (C) electrodes being moved progressively and symmetrically apart. Moving only the C electrodes has two advantages; there are fewer electrodes to move, and with the P electrodes fixed the readings are less affected by any lateral variations that may exist. However, when expansion causes the value of ΔV to become so small that it cannot be measured precisely, the P electrodes are moved much further apart, while keeping the C electrodes fixed; then more readings are taken by extending the C electrodes using the new P electrode positions. Though the values of apparent resistivity (ρ_a) for the two separations of the P electrodes but the same C electrode separation should be the same, in practice they may be different (perhaps because of lateral variation), giving an offset of the apparent resistivity ρ_a, current electrode spacing curve and each section is adjusted to join smoothly to the preceding one. Master curves and modeling programs are available for the Schlumberger array.

$$= \frac{^{2}}{2} \cdot \frac{\Delta}{\,} \qquad (3.12)$$

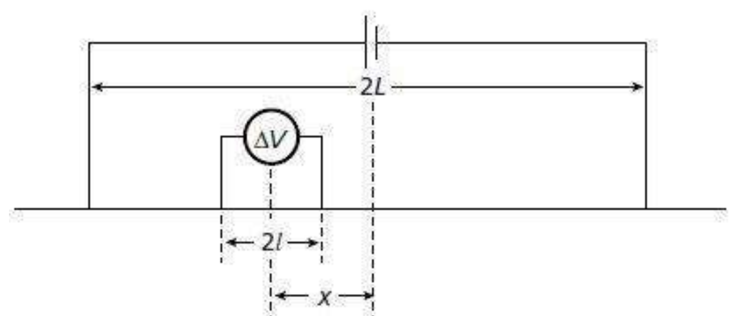

Figure 3.5: Schlumberger configuration (Kearey and Brook 2002)

3.8 VES Data acquisition

Vertical electrical sounding points were located at the zones of high and low conductivity revealed by the VLF interpretation. These points were investigated to an approximated AB/2 spread of 100m, and VES stations were distributed along a regular E-W grid of 500 m × 500 m, with two sounding points on each VLF profile.

Plate IV, shows direct current (DC) resistivity sounding being carried out using ABEM Tarrameter SAS 4000 to generate electrical resistivity data at 12 stations. This instrument allows natural or artificial signals to be measured at considerable low levels, as wells as permits quality penetration and invariable low power consumption.

This was done to encapsulate the electrical resistivity due to variation in the vertical lithology of the subsurface, hence, to estimate the depth to conductive body by inferences.

3.8.1 Data analysis

The data sets from both the VLF and VES investigations were subject to geophysical analysis using Karous-Hjelt filter and WinResist respectively. An electrical conductivity map of the area was developed using Oasis Montaj geophysical tool along with 2D current density sections corresponding to each VLF profile were generated using the Karous-Hjelt filter software.

The Vertical Electrical Sounding data were analysed by plotting on a log-log graph the current electrode separation (AB/2) against the apparent resistivity (ρ_a) to suppress variation at greater depth and to lay emphasis on near surface resistivities.

Both quantitative and qualitative interpretations were done on the results obtained from the analysed data sets hence, inferences and recommendations were drawn.

CHAPTER FOUR

4.0 RESULTS AND DISCUSSION

The results and findings of the entire investigation are discussed in detail in this chapter with a view of attempting to explain in explicit the geophysical and geological characteristics of the surface and subsurface of the study area.

The VLF-EM data acquired contains different non-linear and harmonic noises arising from various sources which tends to make delineation of structures complex, however, for better approximation, filtering technique must be applied to eliminate part of the bias noise of man-made and geological sources to make signal-to-noise ratio smoother. Therefore, Fraser (1969), developed a filtering technique that attenuates long-wavelength signals by removing the Nyquist frequency of noise, and converts high gradients (zero-crossing data) into peaks to enhance the two-dimensional profile.

The VLF-EM data were analyzed and presented in profiles indicating regions of high and low conductivities, putting into cognizance the factors which gave rise to these anomalies. The data were presented in the Fraser filtered format using KHFFILT software so as to eliminate the noise in the data caused by geologic and cultural features of less interest. Corresponding current density pseudo sections were also featured to give a 2D view of the current distributions with an average skin depth of 80 meters.

Peaks corresponding to cross cutting between the real (in-phase) and imaginary (quadrature) in the positive amplitude gave rise to interesting target locations with activities of higher current distributions and those in the negative gave lower current distributions, however, smaller amplitude of In-phase response corresponds to points of relatively good conductor.

Conduction in earth materials are factored by the electronic, ionic and metallic conduction, with each having characteristic means of the conduction processes. Therefore, areas with high conductivity can be inferred to areas with fractures, developed pore spaces (as in sandstone) containing water, or highly mineralised zones containing conducting minerals.

4.1 Results of Very Low Frequency Data

The profile (Figure 4.2) runs from E-W direction and lies between latitude 9.6255^{O}N to 9.6254^{O}N and longitude 6.6082^{O}E to 6.6036^{O}E indicating the highest percentage in amplitude of the in-phase response between 75 m to 125 m (128.9 mS/m) and 300 m to 360 m (56.6 mS/m) (Figure 4.2) with corresponding maximum response of 125% (Figure 4.1) indicating a highly conductive zone which can be inferred to contain conductive minerals due to the high response.

A low conductive structure spans from 150 m to 200 m, with an approximate of 80 m from the surface (Figure 4.2), serving as a host to a conductive body due to facture features.

The evaluation of mineral occurrence in the study area is based on the characteristics of the geoelectric parameters (resistivity and thickness) of the suspected abnormal layer in the area of study.

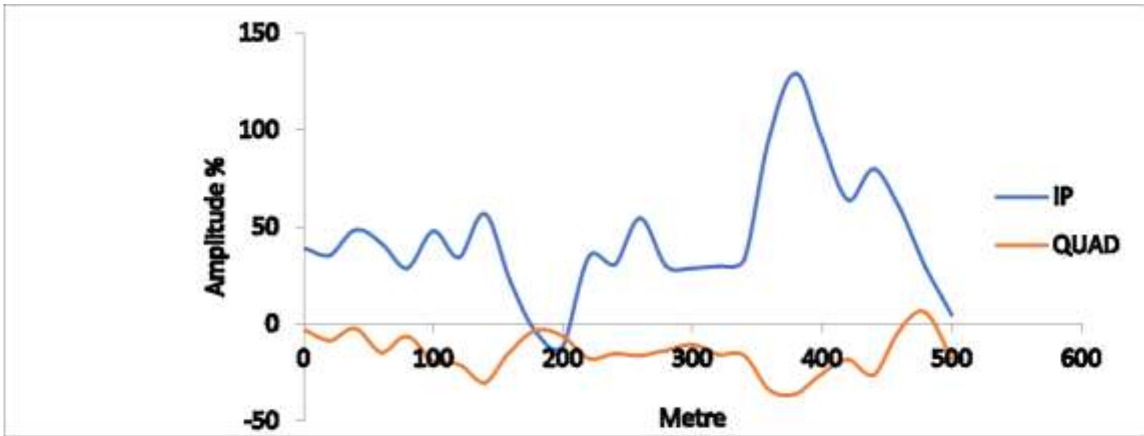

Figure 4.1: VLF1; unfiltered real (IP) and imaginary (Quad)

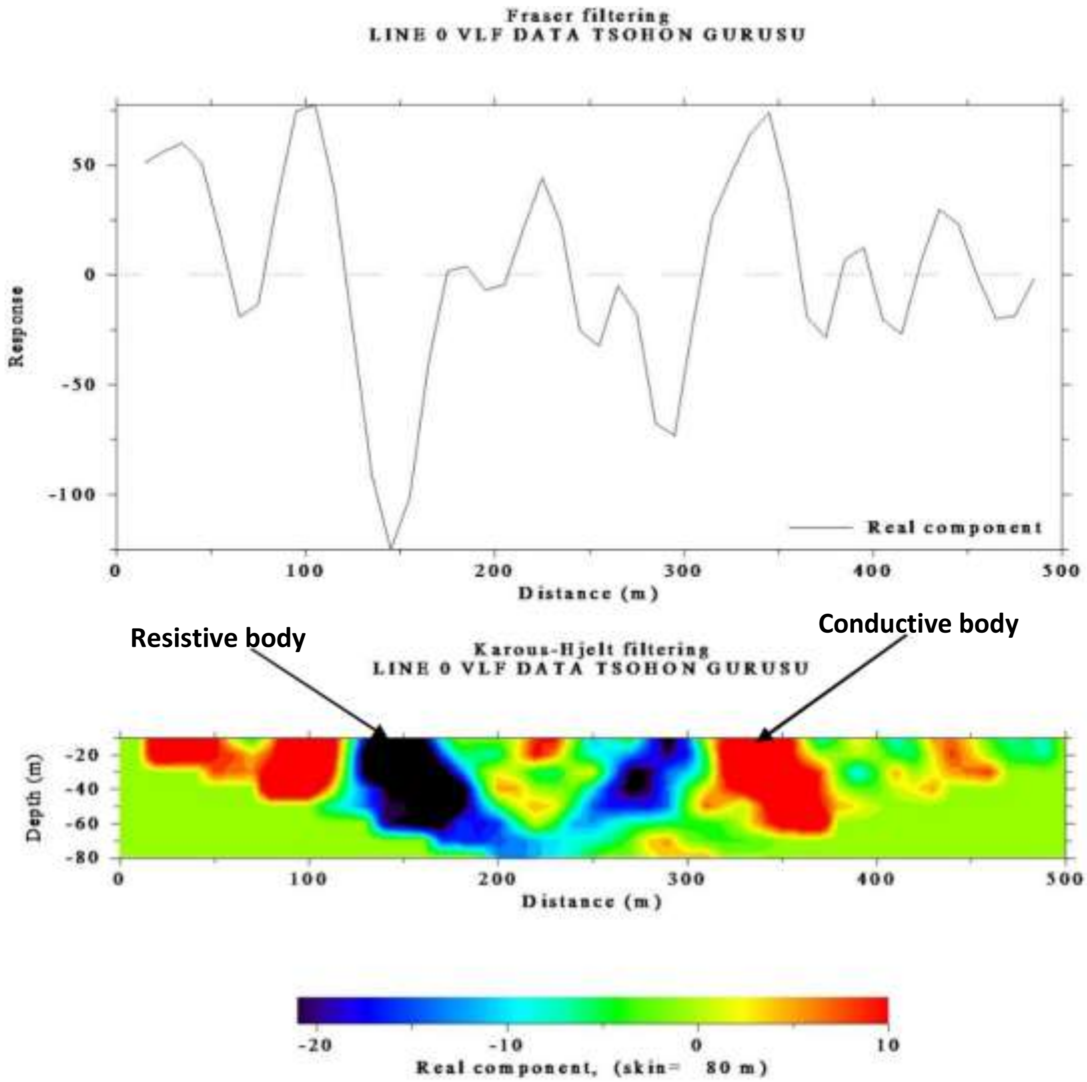

Figure 4.2: Profile 1; Fraser filter graph and 2D current density pseudo section

The profile (Figure 4.4) trend along the W-E direction and lies between 9.6245^{O}N to 9.6246^{O}N and longitude 6.6036^{O}E to 6.6082^{O}E with significant conductivity signatures along 10 m to 40 m (126.5 mS/m), 100m to 175m (98.1 mS/m), 250 m to 310 m (83.2 mS/m) having 110% in-phase response indicative of mineralisation and juxtaposed between low conductive bodies.

Quartzite outcrop in this profile spans from 40 m to 100 m with corresponding low conductive signature (-124 mS/m). There is also an outcrop of granodiorite at 200 m and an outcropping dyke of quartzite with low conductivity (-76 mS/m).

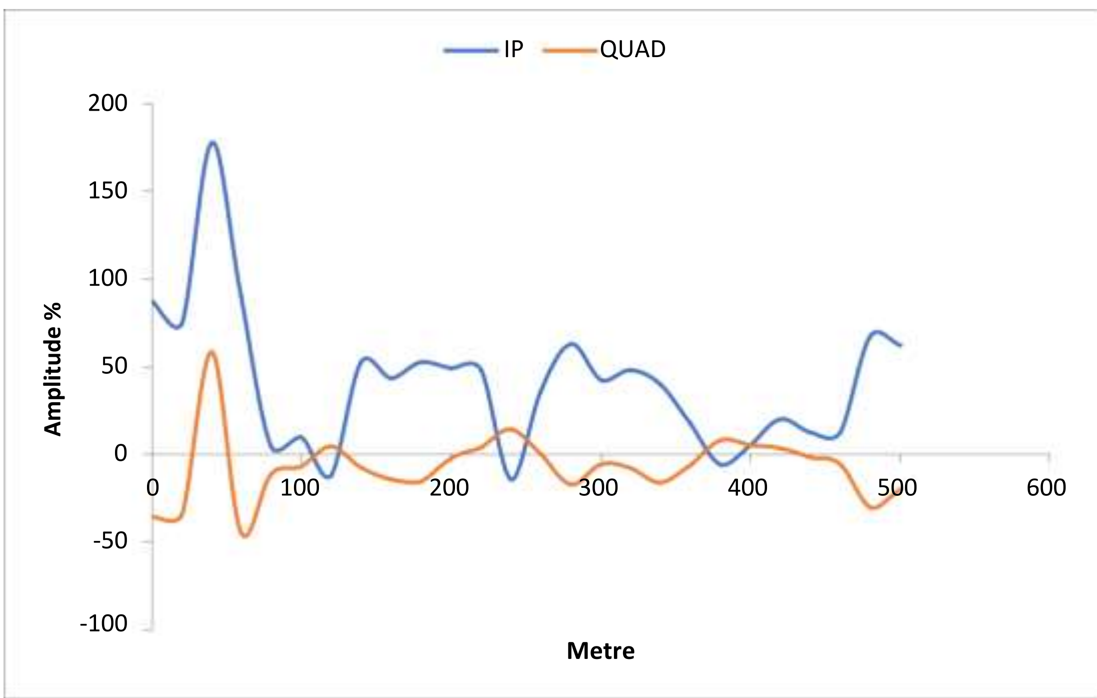

Figure 4.3: VLF2; unfiltered real (IP) and imaginary (Quad)

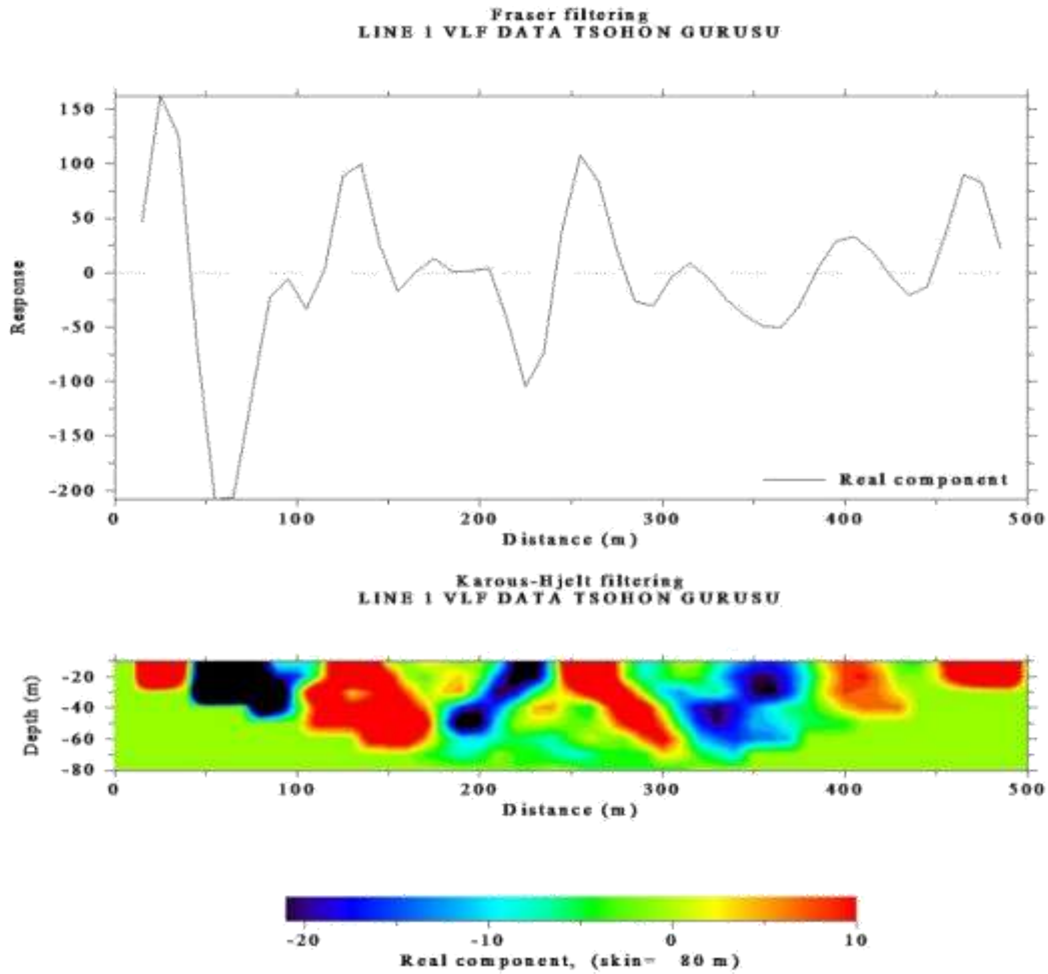

Figure 4.4: Profile 2; Fraser filter graph and 2D current density pseudo section

This profile Figure 4.6, runs along the E-W direction and lies between latitude 9.6237^{O}N to 9.6236^{O}N and longitude 6.6082^{O}E to 6.6036^{O}E with interesting features of fractures and intrusions of high conductive bodies hosted by low conductive bodies, trending NW-SE and spanning from 150 m to 325 m.

The points of inflections of cross-cutting of the real and imaginary component gave rise to the highest conductive signature of 189.4 mS/m as the highest in this profile with in-phase response of 160% lying spanning from 100 m to 150 m with an estimated depth of 60 m from the surface, trending along the NE-SW direction.

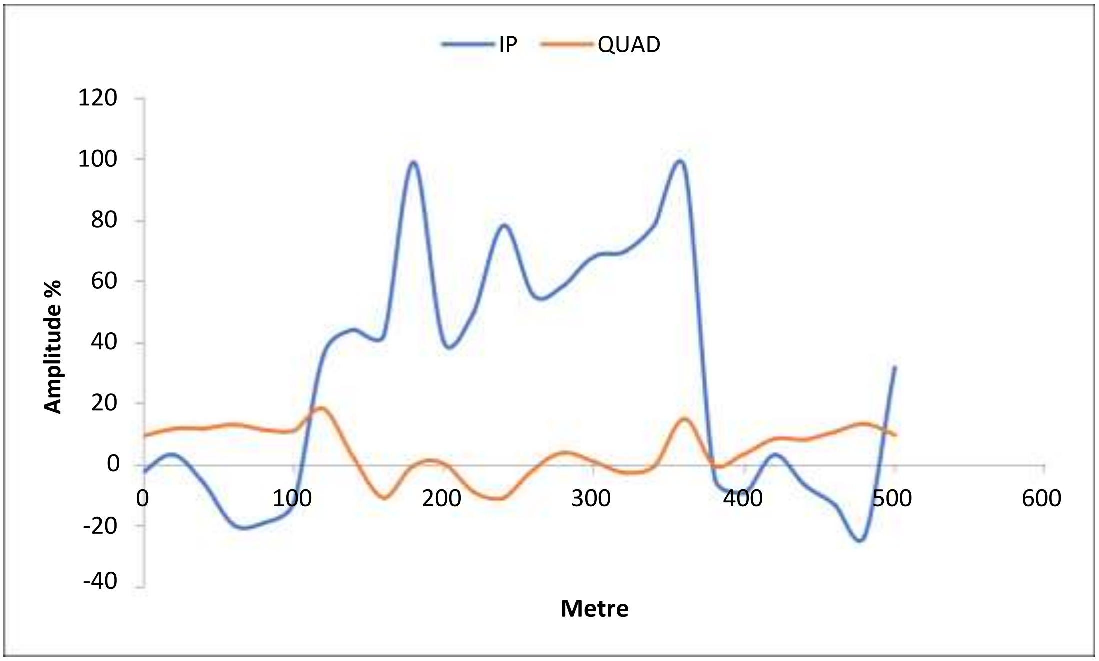

Figure 4.5: VLF3; unfiltered real (IP) and imaginary (Quad

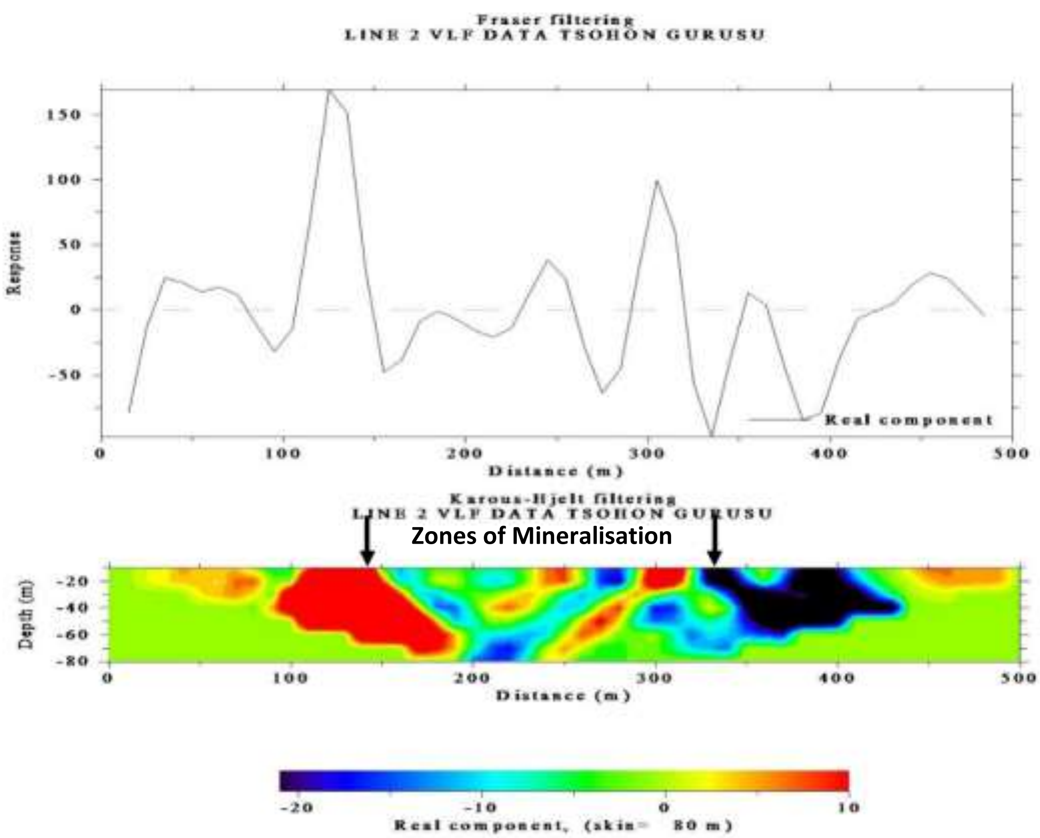

Figure 4.6: Profile 3; Fraser filter graph and 2D current density pseudo section

This profile (Figure 4.8) trends along the W-E direction and lies between latitude 9.6227^{O}N to 9.6228^{O}N and longitude 6.6036^{O}E to 6.6082^{O}E having the highest conductivity from 340 m to 400 m (128.8 mS/m) at an approximate depth of 80 m from the surface with an outcropping low conductive granitic body between 400 m to 430 m serving as an intrusion.

From the start point to 300m, a body of low and intermediately high conductivity seems to dominate, as such, suggest fracture zones susceptible to mineralisation.

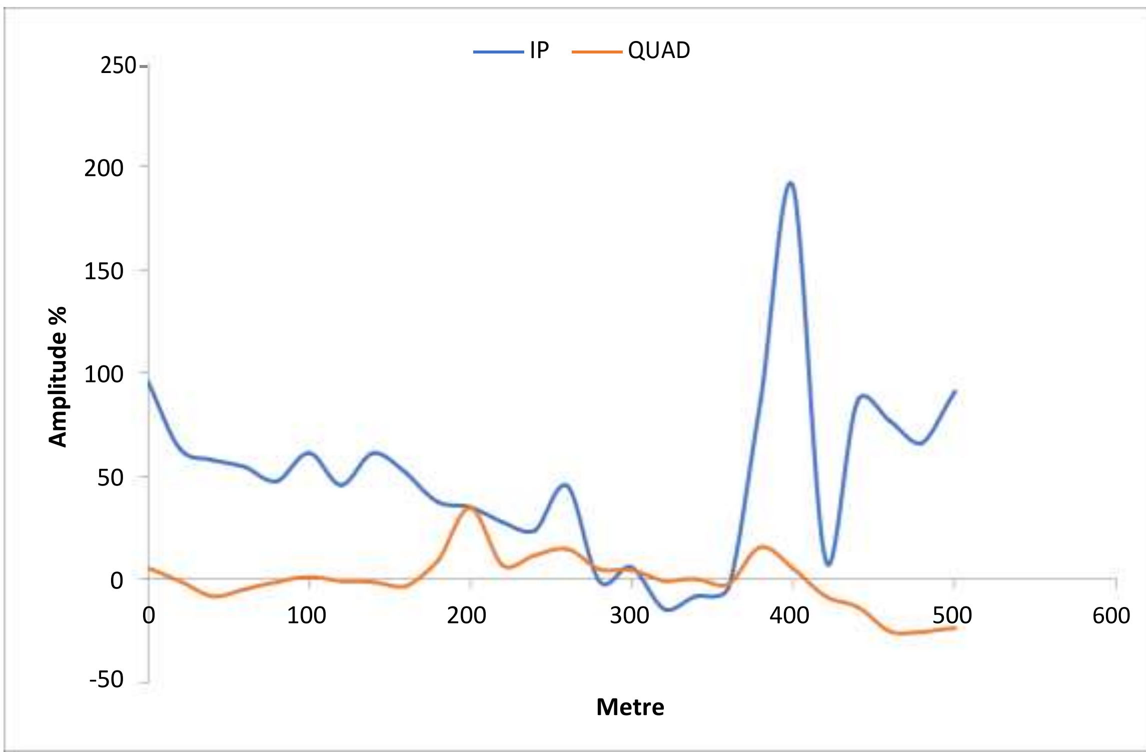

Figure 4.7: VLF4; unfiltered real (IP) and imaginary (Quad)

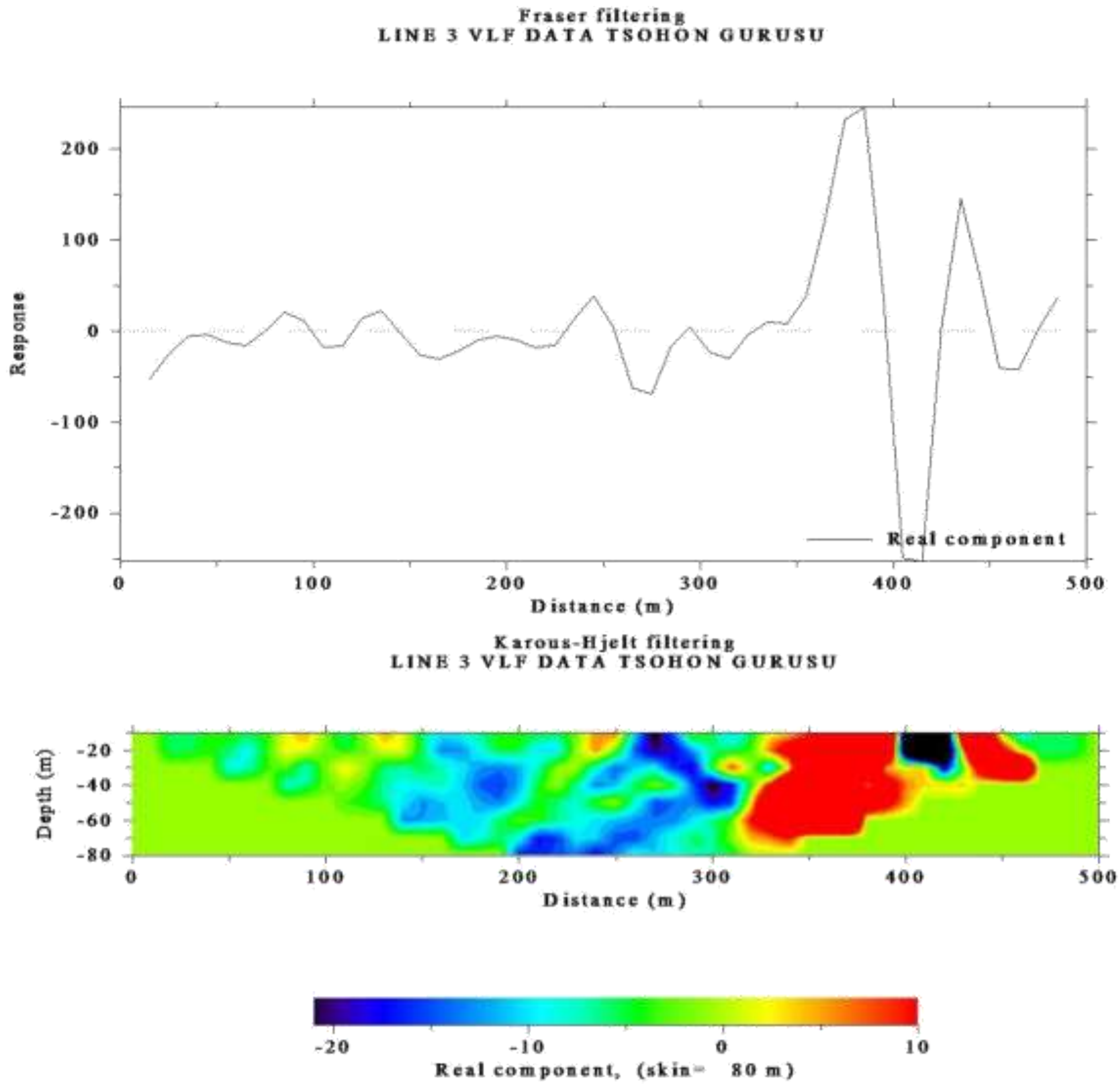

Figure 4.8: Profile 4; Fraser filter graph and 2D current density pseudo section

This profile (Figure 4.10) is along the E-W direction and lies between latitude 9.6219^{O}N to 9.6218^{O}N and longitude 6.6082^{O}E to 6.6036^{O}E. This profile registers the highest conductivity response compared to all the previous profiles as shown in the 2D section, of about 134.3 mS/m at an approximate depth of 60 m from the surface with a NE-SW trend direction and spans from 280 m to 320 m. The general feature is that fracturing units in the profile are highly pronounced.

At distance of 262 m a very low conductive response is shown by a body hosting a high conductive body which can be inferred to be an aquifer or a mineralised zone.

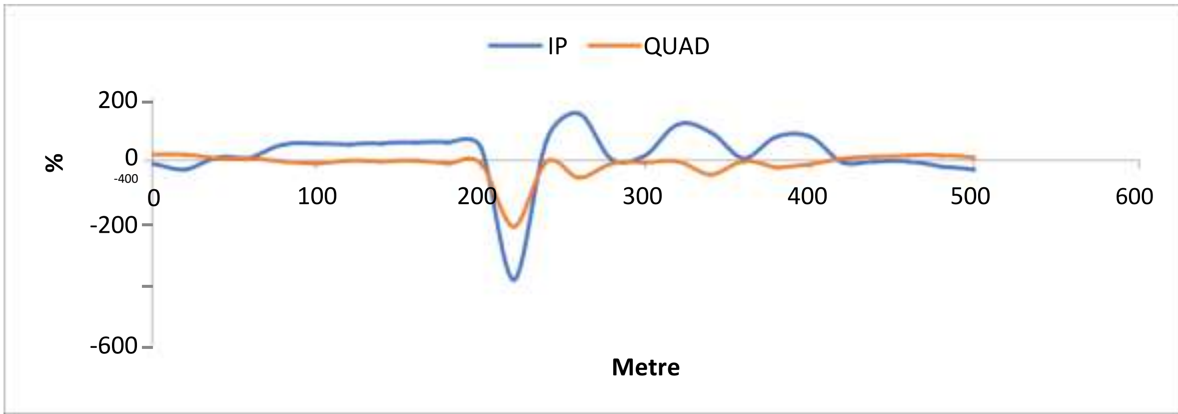

Figure 4.9: VLF5; unfiltered real (IP) and imaginary (Quad)

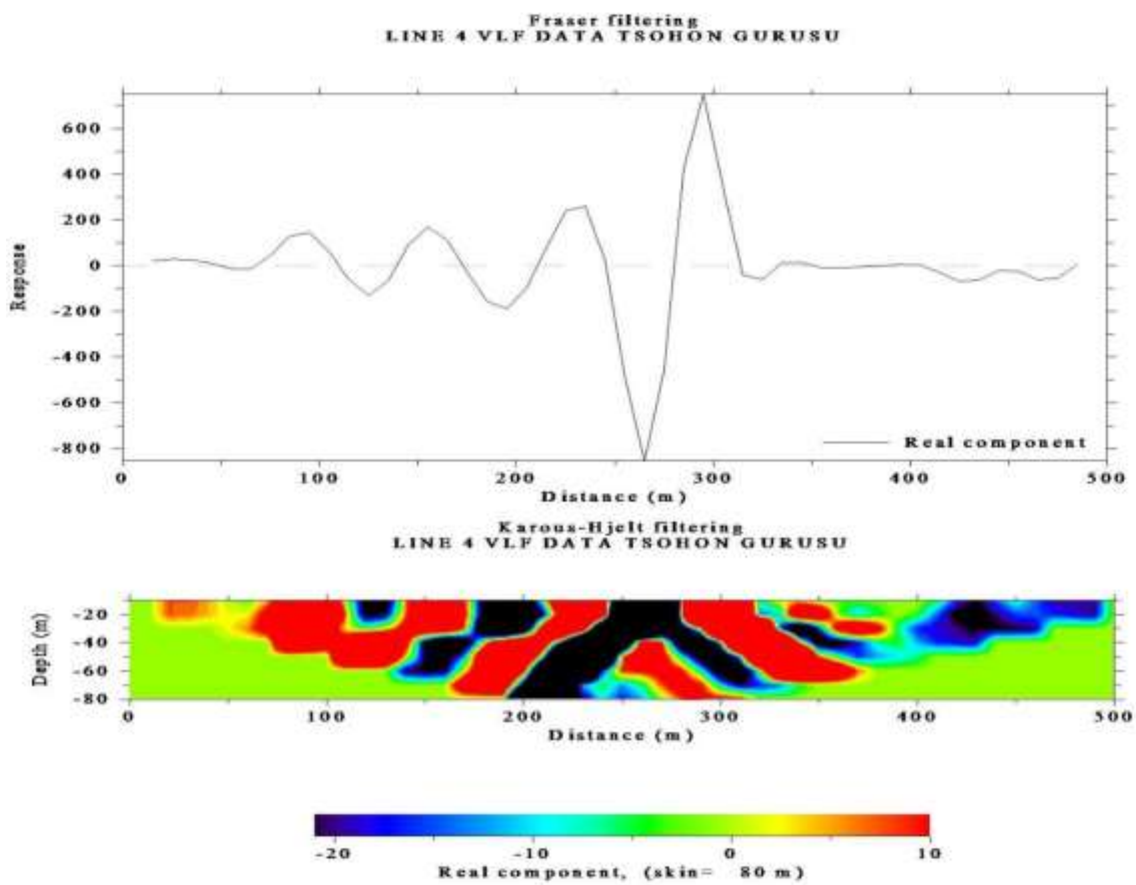

Figure 4.10: Profile 5; Fraser filter graph and 2D current density pseudo section

This profile Figure 4.12, runs on the W-E direction and lies between latitude 9.6209^{O}N to 9.6210^{O}N and longitude 6.6037^{O}E to 6.6082^{O}E. The highest conductivities response is shown at 450 m (120.3 mS/m) and 200m (127.6 mS/m) on the profile with the least conductive response at 300m (-122.5 mS/m) corresponding to a geologic outcrop of quartzite which is highly resistive, as such, hand specimen of rock samples within this profile indicated possible presence of non-conductive minerals with economic potential.

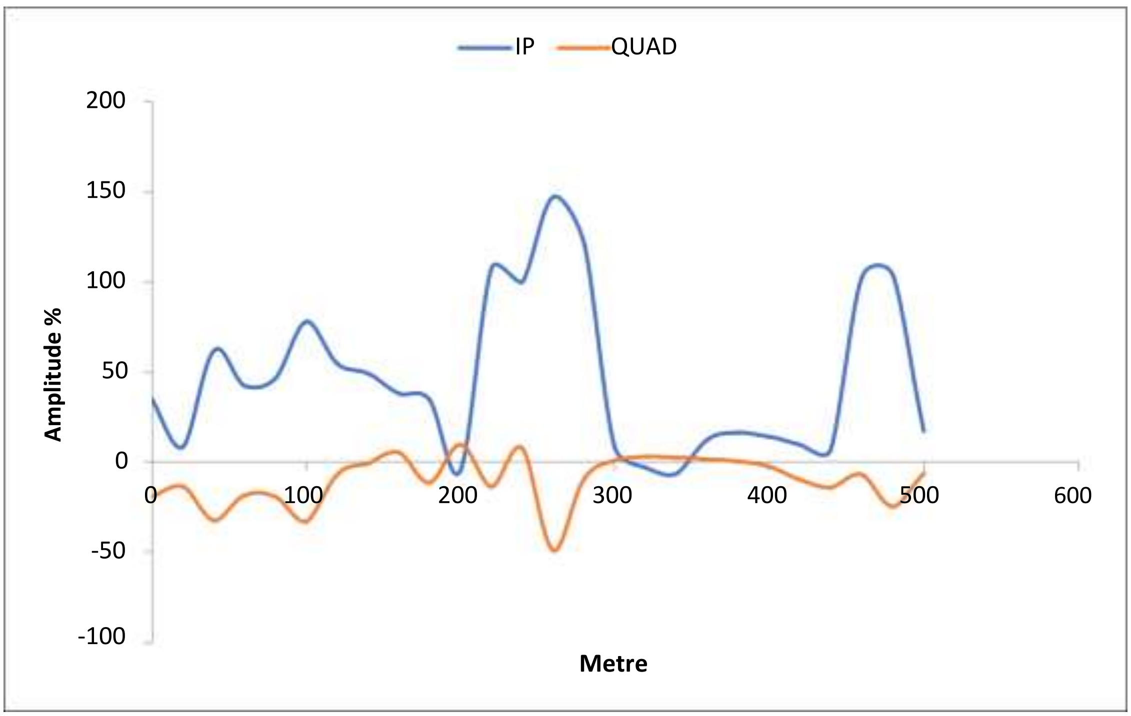

Figure 4.11: VLF6; unfiltered real (IP) and imaginary (Quad)

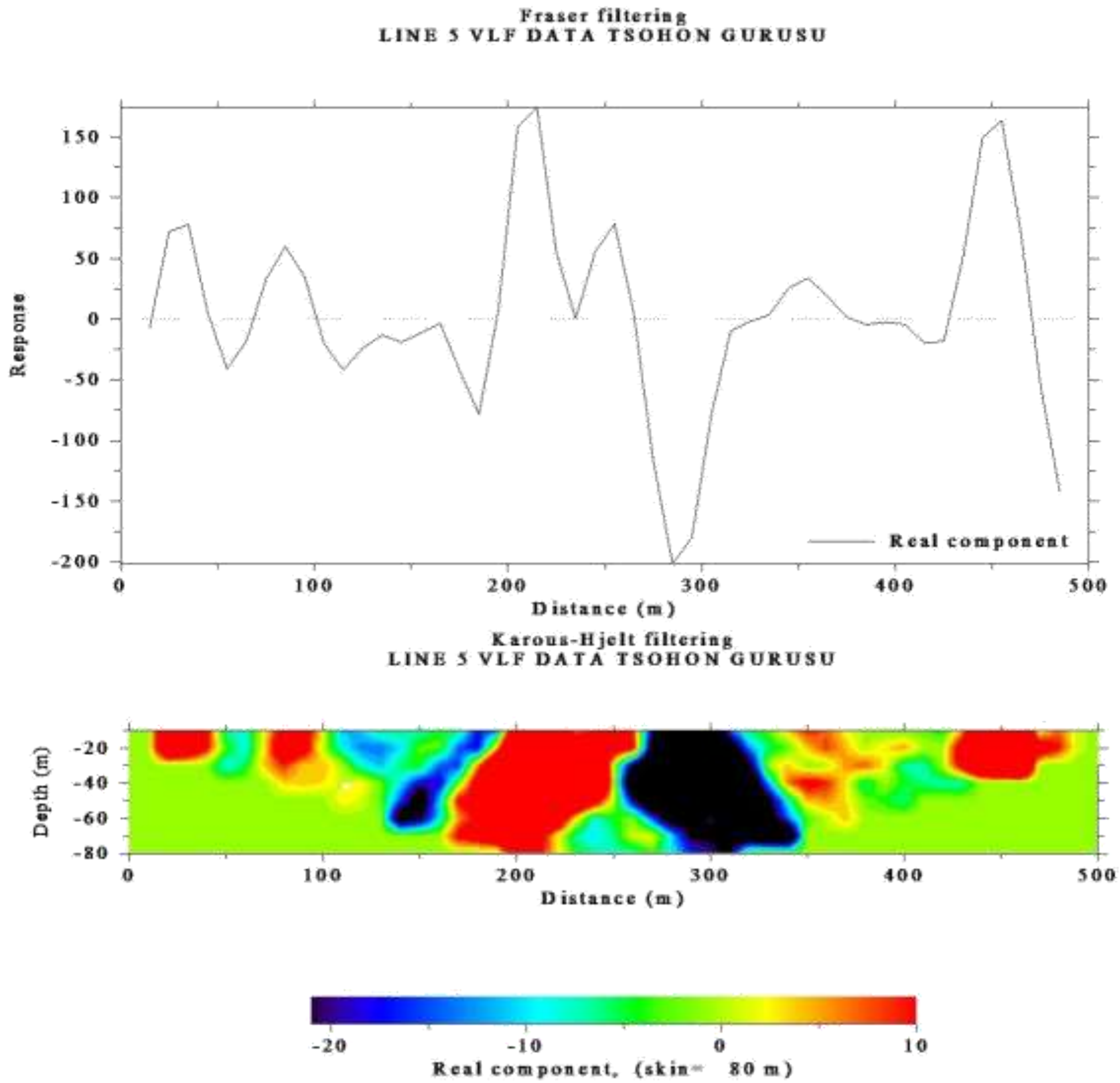

Figure 4.12: Profile 6; Fraser filter graph and 2D current density pseudo section

Figure 4.13 is the total conductivity map obtained from the combined VLF data of the study area. It indicates regions of high and low conductivity values within the ranges of 135.5 mS/m to -136.7 mS/m respectively. The major conductivity trends lies along the NE-SW direction, with fringes of conductive structures as intrusions in areas of low conductivity (high resistivity).

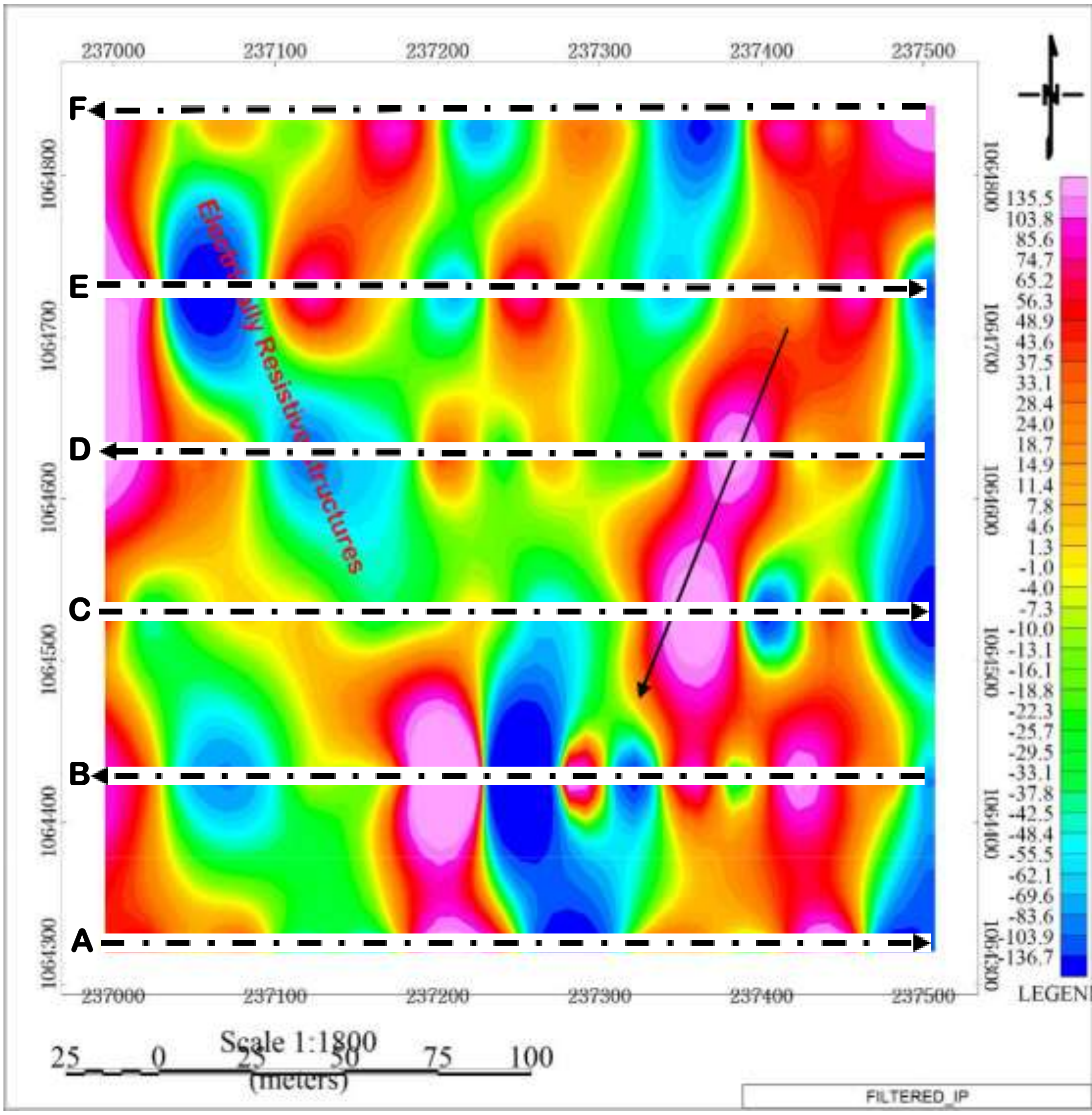

Figure 4.13: Generalised conductivity map of the study area showing profile A – F with their corresponding direction

4.3 Vertical Electrical Sounding Data Analysis

Electrical conductivity of mineral rocks of interest was specified from the Very Low frequency Electromagnetic data sets and 12 Vertical Electrical Sounding points were established, and Schlumberger Configuration of Vertical sounding field curves were generated which can be interpreted qualitatively using simple curve shapes, semi quantitatively with graphical model curves, or quantitatively with computer modelling (Reynolds, 2011).

The results obtained from the comparison of the data and the master curves yielded different types of curve fittings, described by the plotted graphs of the VES data. Qualitative analysis of the VES data set enhanced the descriptions of the subsurface layers.

Figure 4.14 reveals geo-electric layers under VES 01 sounded on the low conductive structure, yielding a H-type curve with topsoil of resistivity values of 23.3 Ohm-m and thickness of 1.8 m on VLF profile 1 Figure 4.2, possibly consisting majorly of sandstone underlain with clay. The topsoil is underlain by undifferentiated schist with quartzite intrusions of resistivity 15.8 Ohm-m and thickness 4.3 m and serves as possible mineralised zones. An anomalous layer with resistivity value 2740.7 Ohm-m, considered as the fresh basement of mainly granitic composition.

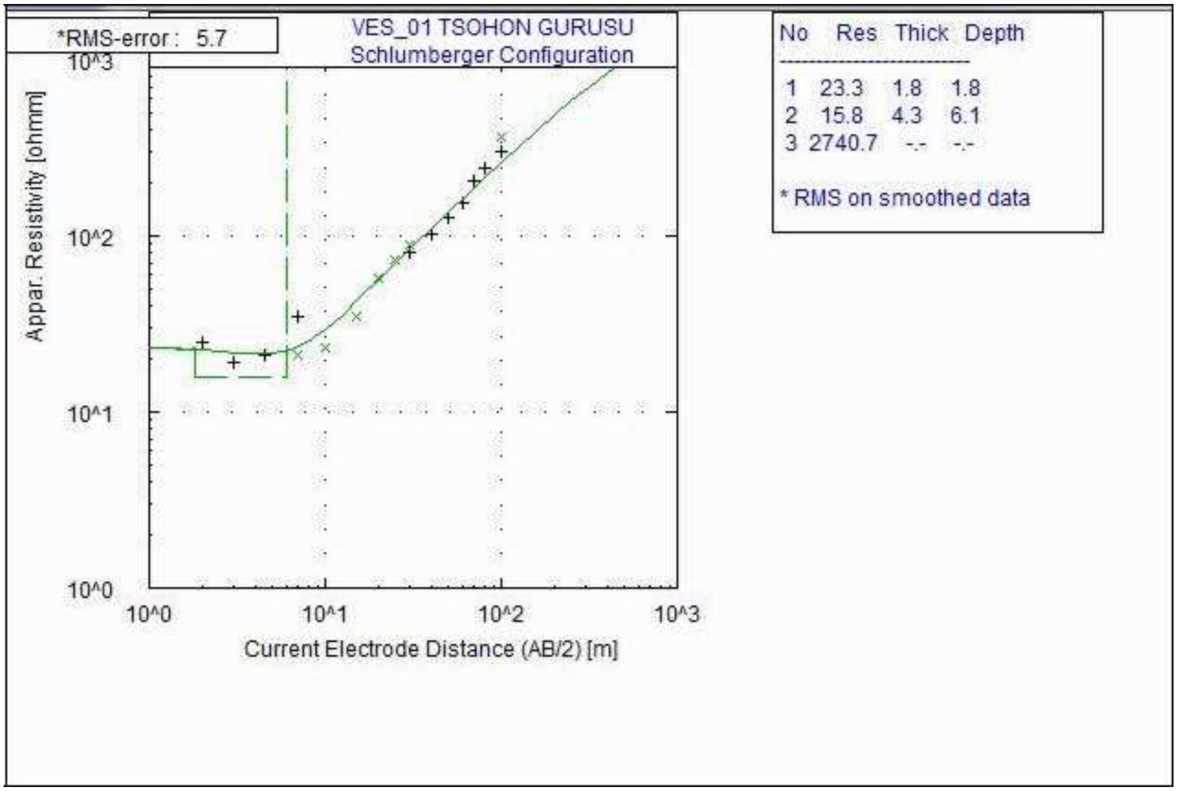

Figure 4.14: Vertical electrical sounding 01

The VES 02; Figure 4.15, sounded on VLF profile 1 Figure 4.2, showed three-layered H-type curve formations which were interpreted as top soil consisting of Sandstone and clay, highly fractured metamorphic rock (schist), with fringes of conductive materials and granitic weathered to fresh basement, with apparent resistivity of 28.0 Ohm-m, 18.0 Ohm-m and 464.1 Ohm-m respectively.

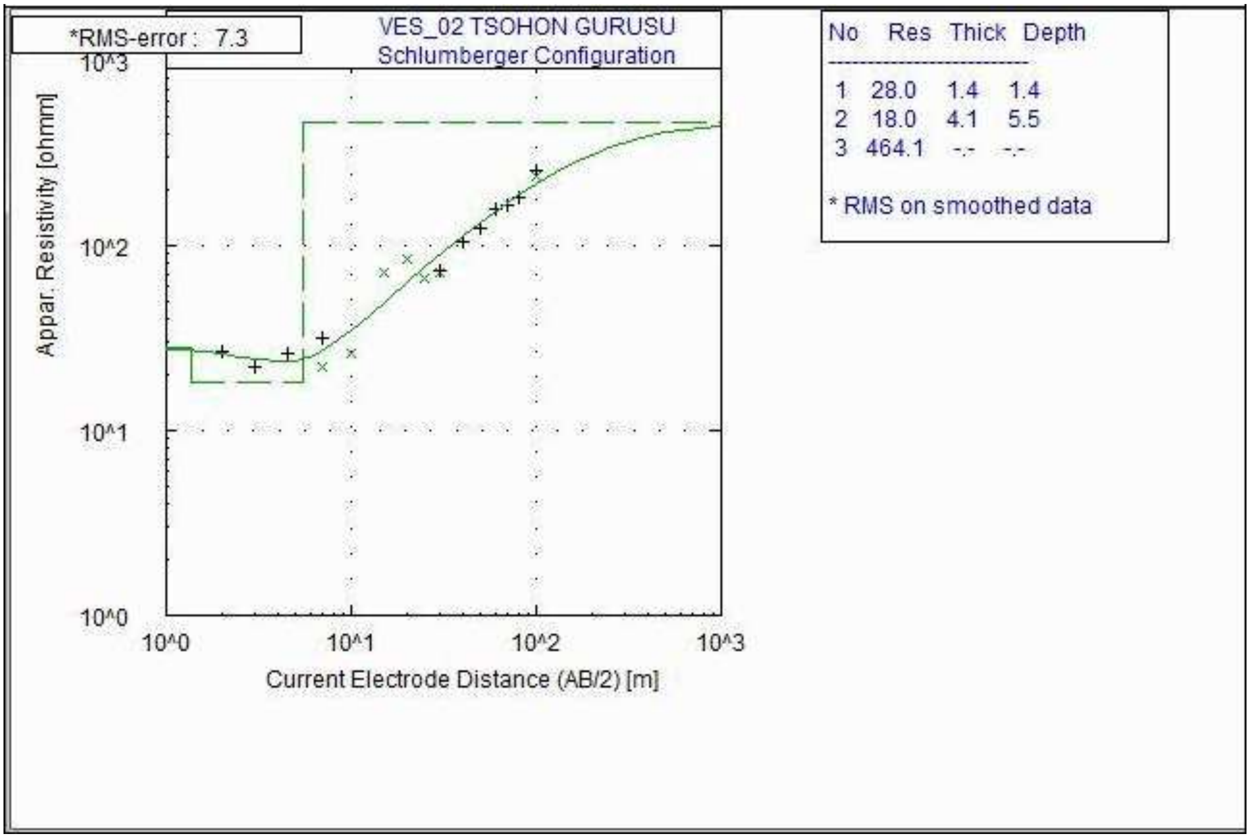

Figure 4.15: Vertical electrical sounding 02

The VES_03; Figure 4.16, on VLF profile 2 Figure 4.4, is characterised by a three layered geo-electric surface with a H-type curve of 70.6 Ωm resistivity of top loosed soil comprising of quartzites and sasndstone, underlain by a lower resistive layer of 26.6 Ωm with a thickness of 11.9 m believed to be sandy-clay at a depth of 12.8m followed by weathered to fresh basement granitic rock of 2309.3 Ωm.

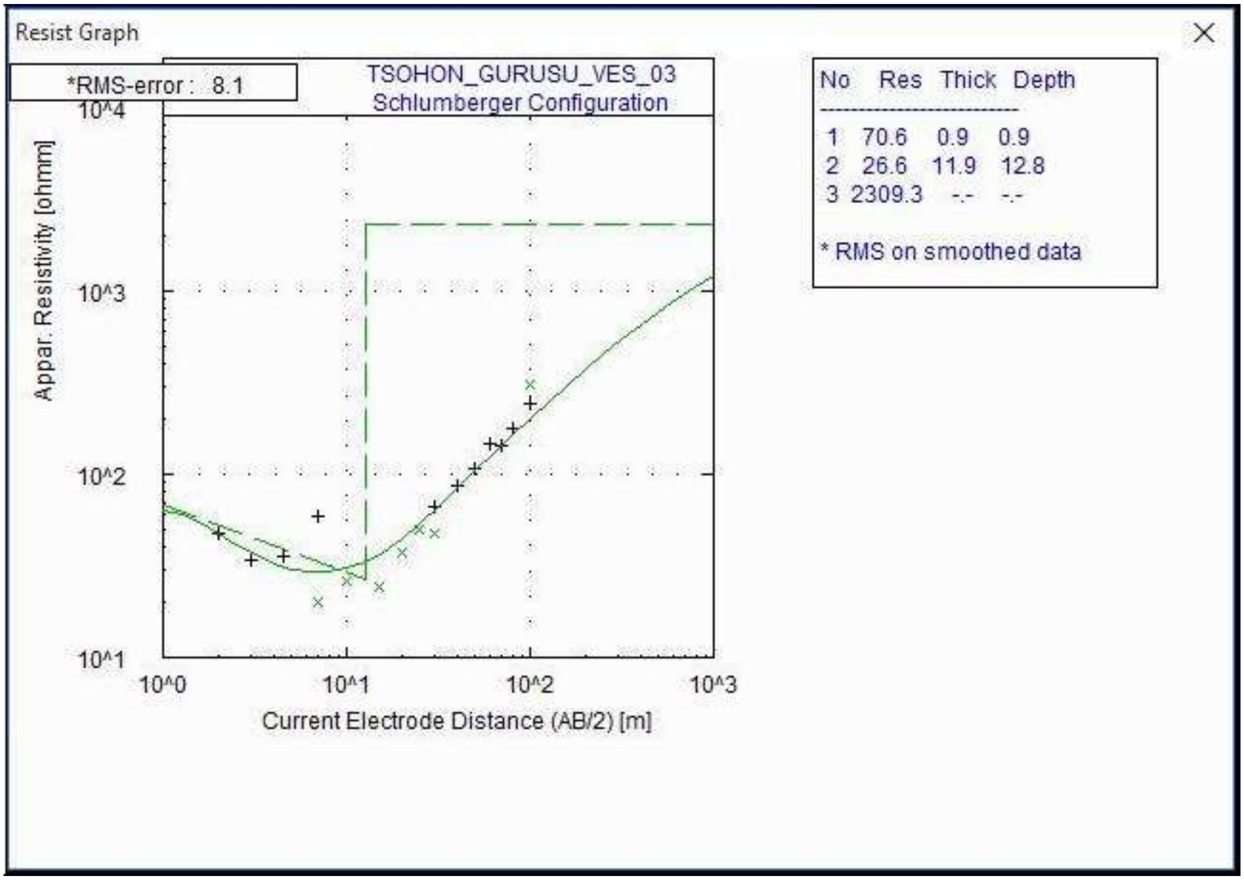

Figure 4.16: Vertical electrical sounding 03

VES_04 (Figure 4.17) corresponds to the VLF profile 2; Figure 4.4, to a distance of 150 m ground measurement with a conductive response of over 100% which indicates possible presence of conductive body/mineral layered on a three geo-electric section of an H-type curve with a topsoil of 20.0 Ωm with 1 m thickness at a depth of 1 m, 10.1 Ωm composed of clayey mineral layer at a depth of 5.9 m with a thickness of 4.9 m followed by a high resistive rock of 3195.5 Ωm.

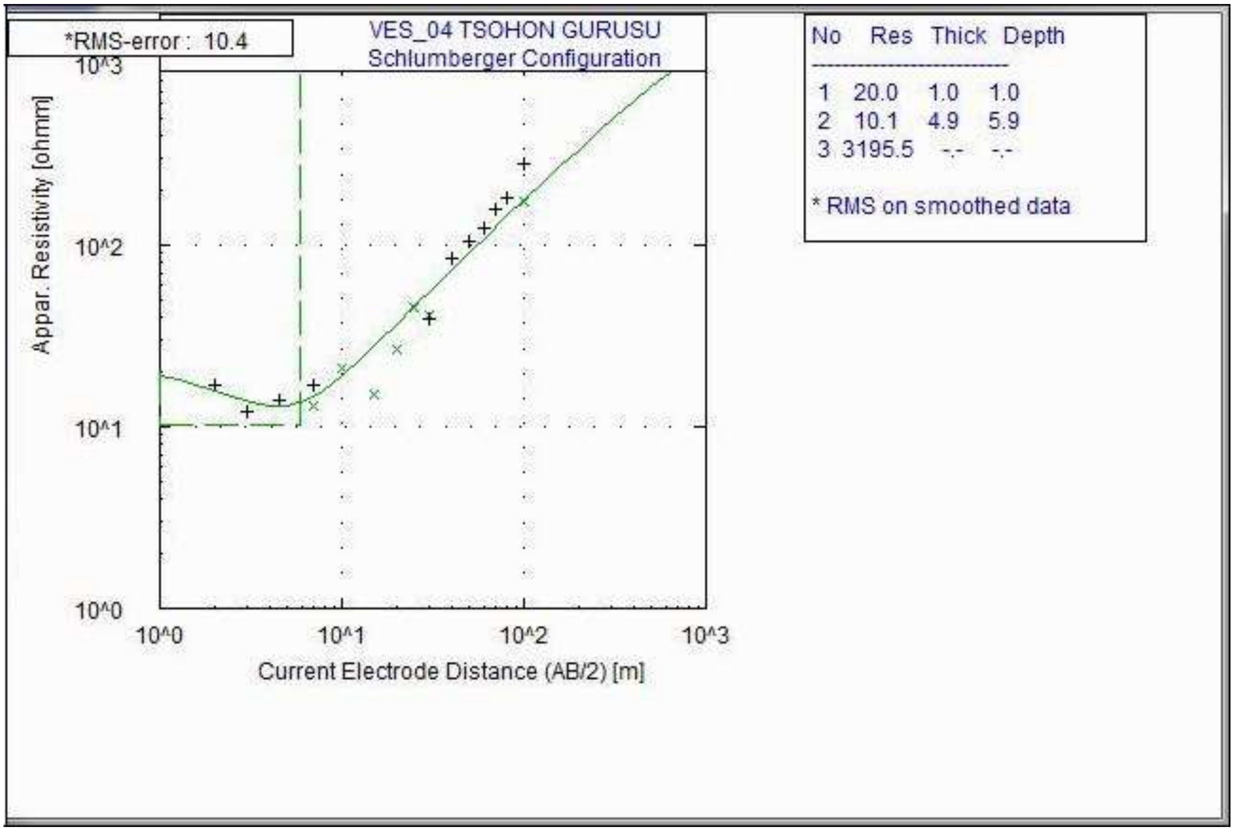

Figure 4.17: Vertical electrical sounding 04

VES_05; Figure 4.18 was sounded on a conductive surface as indicated on the VLF profile 3; Figure 4.6 on a land measurement of 133 m and yielded an H-type curve of three geo-electric section with a relatively low resistive topsoil of 14.4 Ωm with a thickness of 2.3 m at a depth of 2.3 m and a lower resistive layer of 10.1 Ωm at a depth of 9.9 m with a thickness of 7.6 m serving as a possible mineralized zone of conductive materials followed by a weathered to fresh basement formation of 713.0 Ωm.

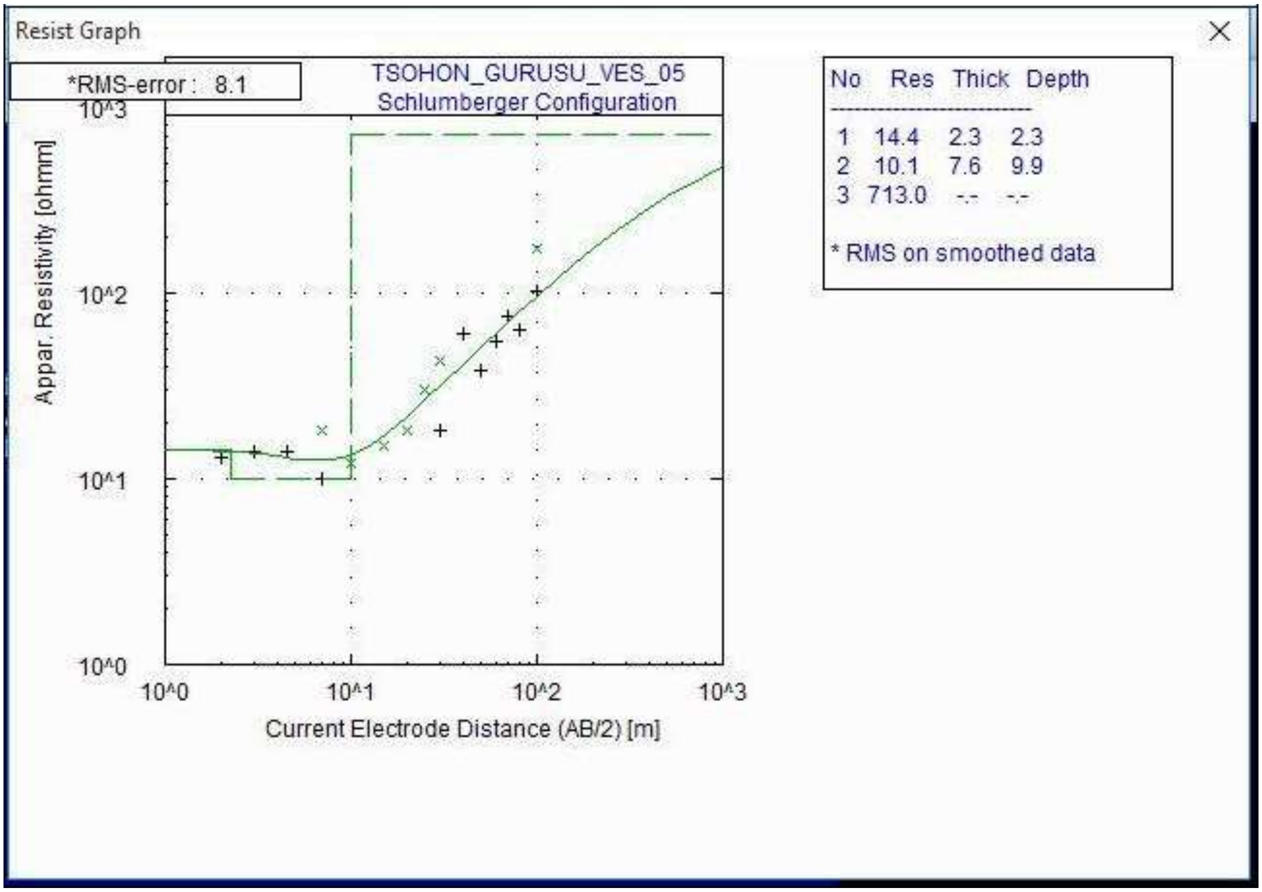

Figure 4.18: Vertical electrical sounding 05

VES_06; Figure 4.19, was sounded on a highly resistive dyke as shown from the VLF profile 3; Figure 4.6, with an initial resistivity of 66.7 Ωm of thickness 0.8 m, at a depth of 8.0 m with an abruptly lower resistivity of 23.8 Ωm with a thickness of 14.4 m at a depth of 15.2 m indicating a possible fractured zone of mineralisation of conductive materials or an aquiferous layer which is underlain by a body of 1470.3 Ωm. This sounding gave rise to a three layered geo-electric section of an H-type curve.

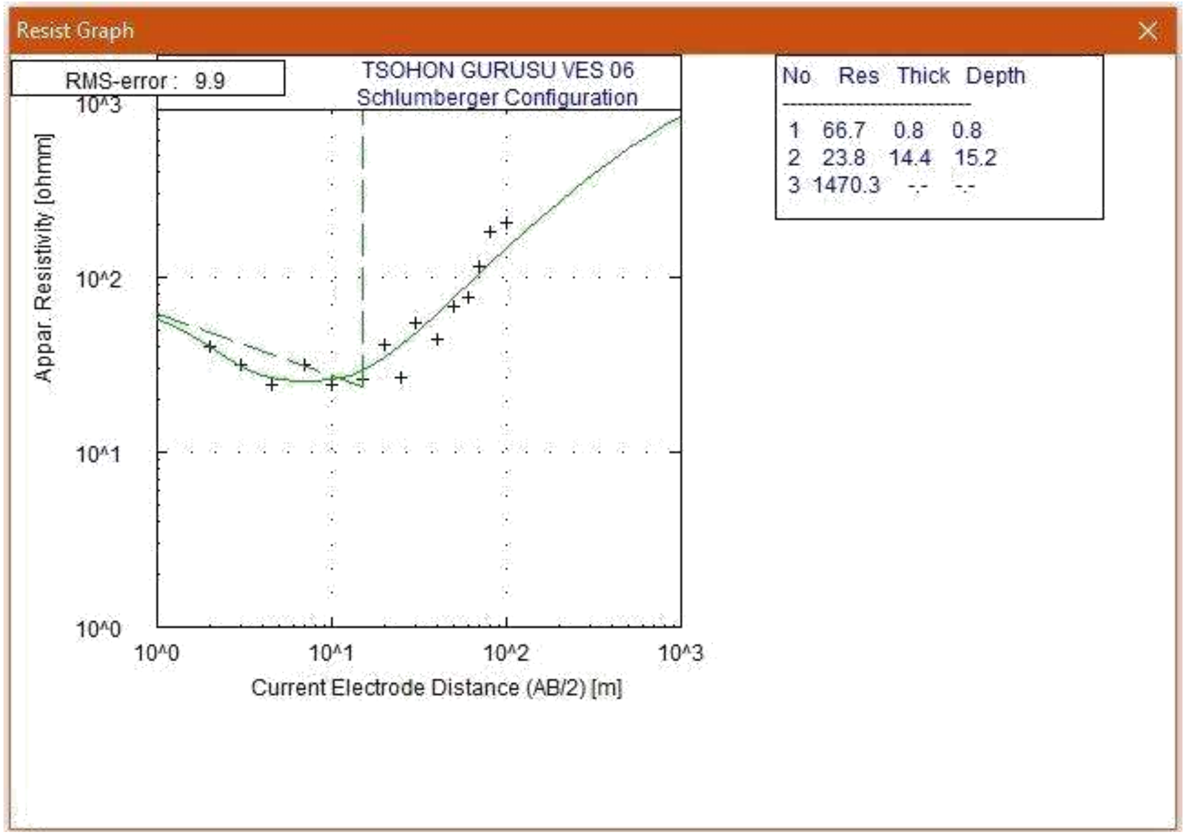

Figure 4.19: Vertical electrical sounding 06

VES_07; Figure 4.20 is characterised by various anomalous bodies and exhibits H-curve type indicating intrusions and fractures at the point of sounding. Having topsoil layer resistivity of 15.9 Ωm of thickness 0.9 m at a depth of 0.9 m, at a depth of 11.4 m is lain a 42.9 Ωm rock body of thickness 10.6 m believed to be an intrusion of metamorphic rock (undifferentiated schist). The VLF profile 4 shows fringes of conductive bodies (clayey minerals) that are disseminated and shows a VLF Figure 4.8, response of 60.9% indicative of mineralisation. This layer is then underlain by a weathered to fresh basement of resistivity 1523.3 Ωm.

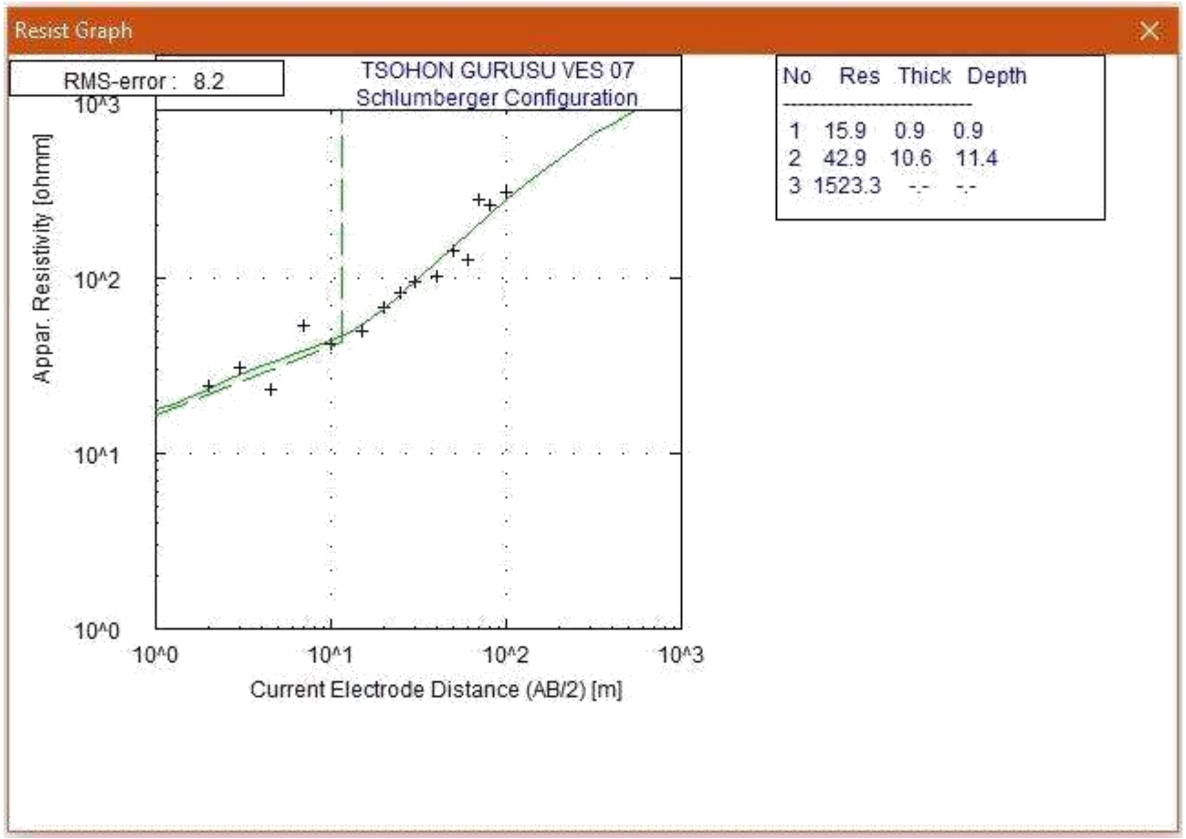

Figure 4.20: Vertical electrical sounding 07

VES_08; Figure 4.21, gave rise to an A-type curve and a three layered geo-electric surfaces of topsoil resistivity of 18.6 Ωm at a depth and thickness of 3.2 m comprising chiefly of saturated sandstone underlain by 81.1 Ωm resistive rock considered to be metamorphic rock (undifferentiated schist) with thickness of 113.2 m at a depth of 6.6 m, minimal activities mineralisation are considered to possibly occur between the second and third layer in the geo-electric section due to the low VLF Figure 4.8, response at this point of sounding. The third layer is predominantly dominated by weathered to fresh basement of 3195.2 Ωm resistivity.

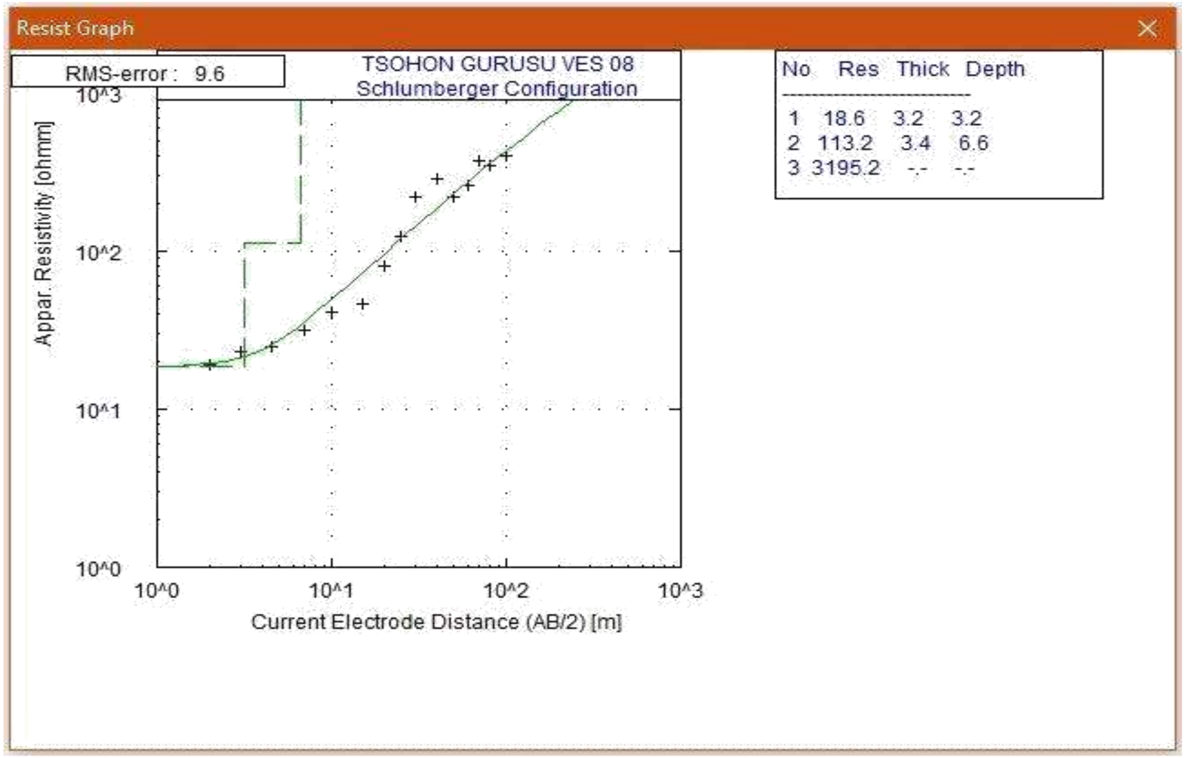

Figure 4.21: Vertical electrical sounding 08

VES_09; Figure 4.22 is characterised by majorly three layered geo-electrical sections of an A-type curve of topsoil resistivity of 71.6 Ωm at a depth and thickness of 0.9 m consisting of loosed sandstone bed and quartz rubbles, underlain by clay and highly weathered undifferentiated schist of resistivity 86.3 Ωm at depth and thickness of 6.5 m and 5.6 m respectively. This layered is also underlain by weathered to fresh basement of 566.6 Ωm intruded by a highly conductive body considered to be a possible mineralisation zone as indicated on the VLF profile 5; Figure 4.10, at a depth of 40 m to 80 m.

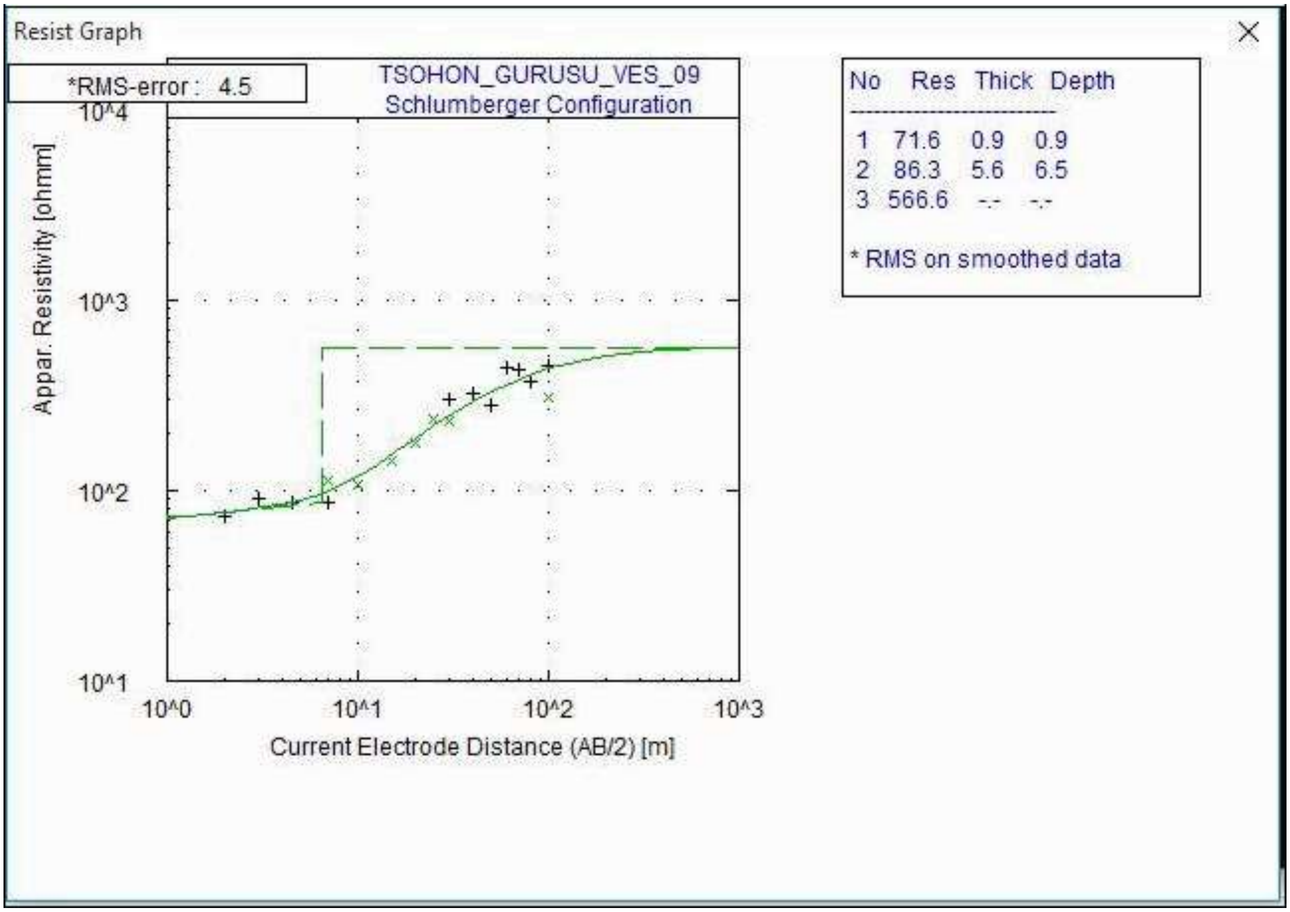

Figure 4.22: Vertical electrical sounding 09

VES_10 corresponds to the VLF profile 5; Figure 4.10, at a ground distance measurement of 165 m W-E with the sounding giving rise to an H-type curve of three major geo-electrical sections, with highly saturated and conductive topsoil layer of 10.2 Ωm resistivity with depth and thickness of 5.7 m considered to be a possible zone of mineralisation with VLF response of over 180%, and underlain by a highly resistive body of 2196.8 Ωm.

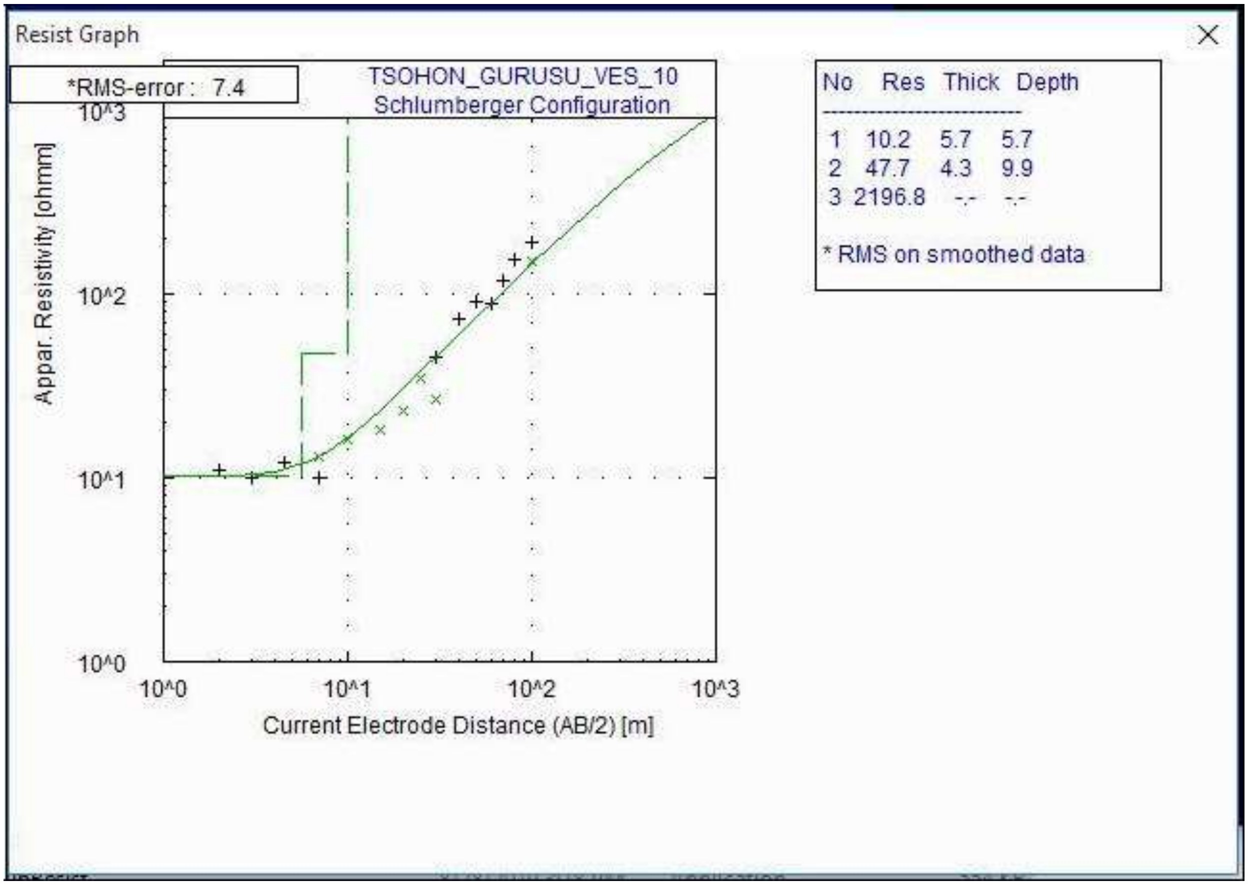

Figure 4.23: Vertical electrical sounding 10

VES_11; Figure 4.24, is located on profile 6; Figure 4.12 on a ground measurement of 200 m W-E and is characterised by a HK-type curve with five major geo-electrical sections with intermediate low and high resistivity owing to multiple zones of possible mineralisation, with topsoil resistivity of 78.1 Ωm of depth and thickness of 1.0 m accompanied by a layer of low resistivity of 21.7 Ωm with corresponding depth and thickness of 4.6 m and 3.6 m respectively having over 140% VLF response indicating possible zone of mineralisation. This layer is underlain by a highly resistive body of 944.9 Ωm resistivity of depth and thickness of 24.1 m and 19.5 m respectively which is considered to be granitic in nature with an underlying layer of intrusive of lower resistivity of 218.5 Ωm at a depth and thickness of

61.6 m and 37.4 m respectively. Followed by a highly fractured/mineralized zone of resistivity of 102.3 Ωm.

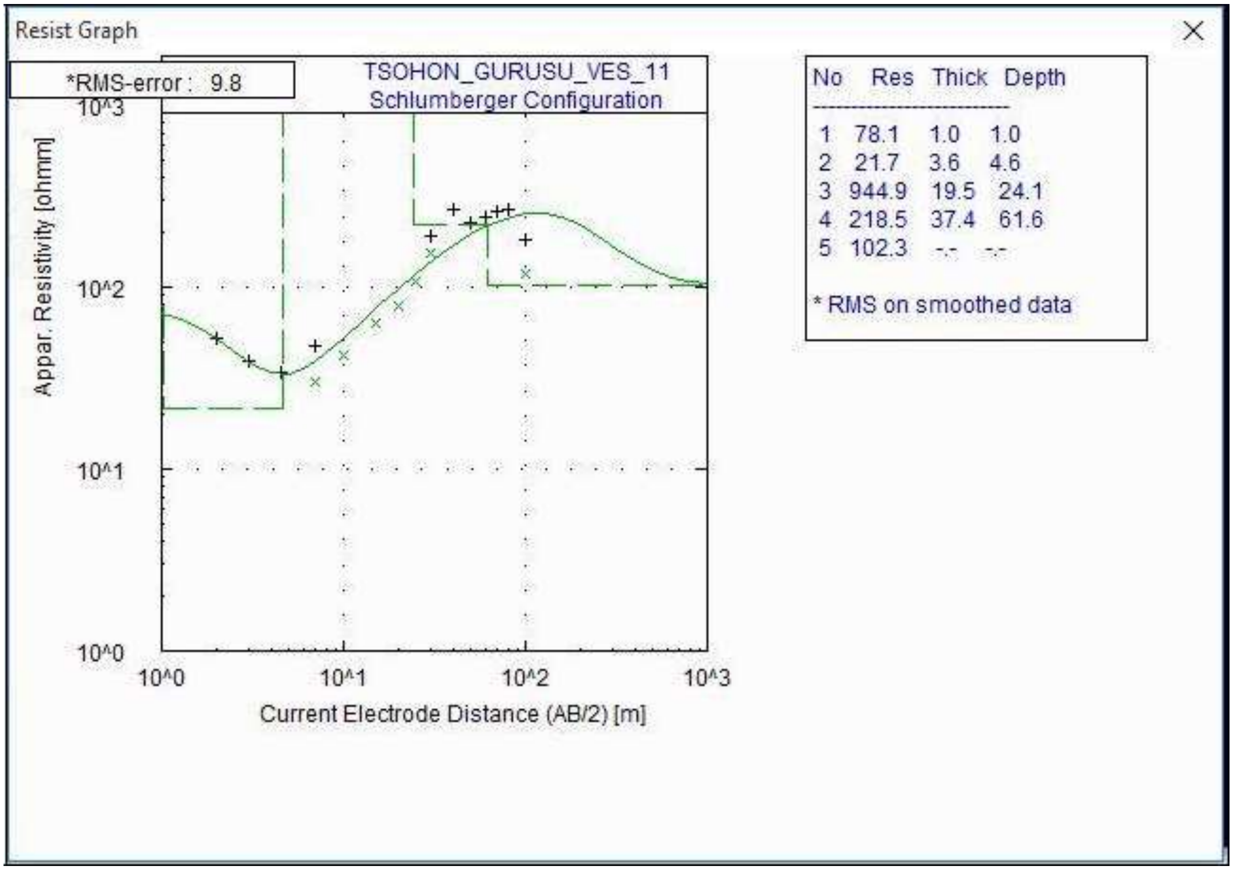

Figure 4.24: Vertical electrical sounding 11

VES_12; Figure 4.25, sounded on VLF profile 4.12, is characterised by majorly three layered geo-electric sections of an H-type curve of topsoil resistivity of 154.6 Ωm, thickness and depth of 1.0 m, underlain by a body of resistivity 97.5 Ωm of thickness and depth of 8.6 m and 7.6 m respectively, followed by layer of higher resistivity of 534.0 Ωm considered as weathered to fresh basement granitic rock.

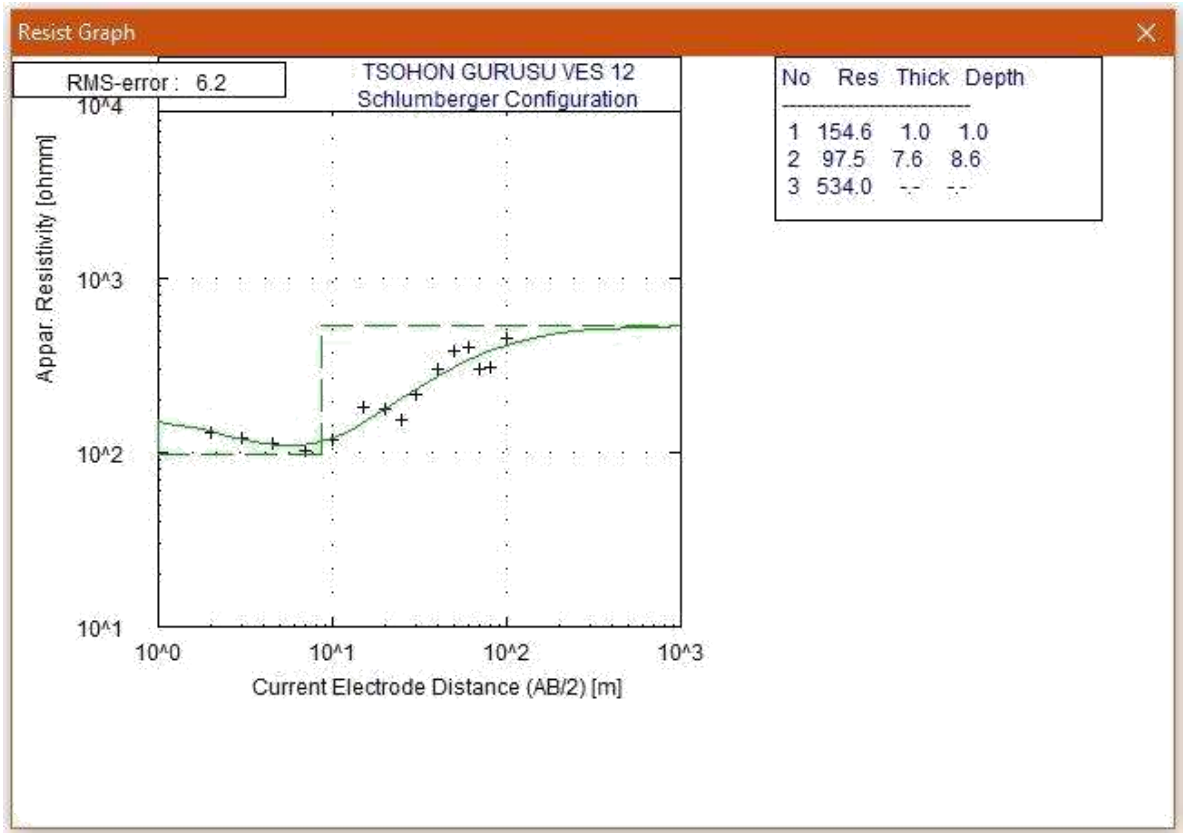

Figure 4.25: Vertical electrical sounding 12

The generalised resistivity maps of three different layers were obtained. The resistivity map of the layer 1; Figure 4.26 obtained at an approximate depth of 9 m was compared with the generalised conductivity map; Figure 4.13 of the study area for conductivity and resistivity similarities and general structural trend.

Figure 4.26, is the generalised VES resistivity map of the first layer of the 12 sounded points, which indicates a general structural trend of NE-SW corresponding to the generalised conductivity map of the area (Figure 4.26). This layer map is estimated at an approximate depth and layer thickness of 2 m, showing highly resistive structure at VES 1.

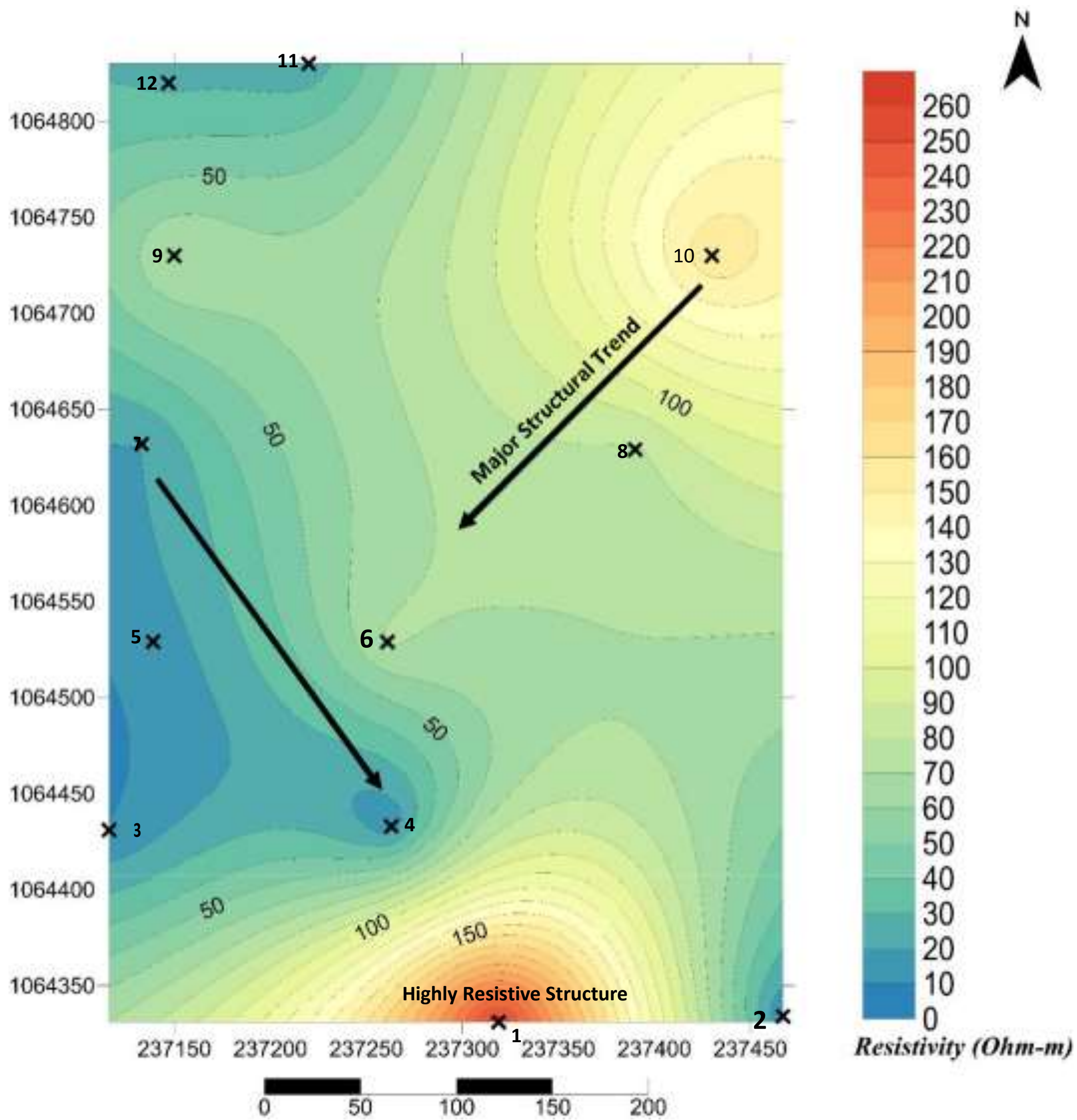

Figure 4.26: Generalised VES resistivity map of layer 1

Figure 4.27 is the generalised VES resistivity map of second layer, indicating location of resistive structure at an approximate depth of 9 m and layer thickness of 8 m. The trend of the major structure is NE-SW.

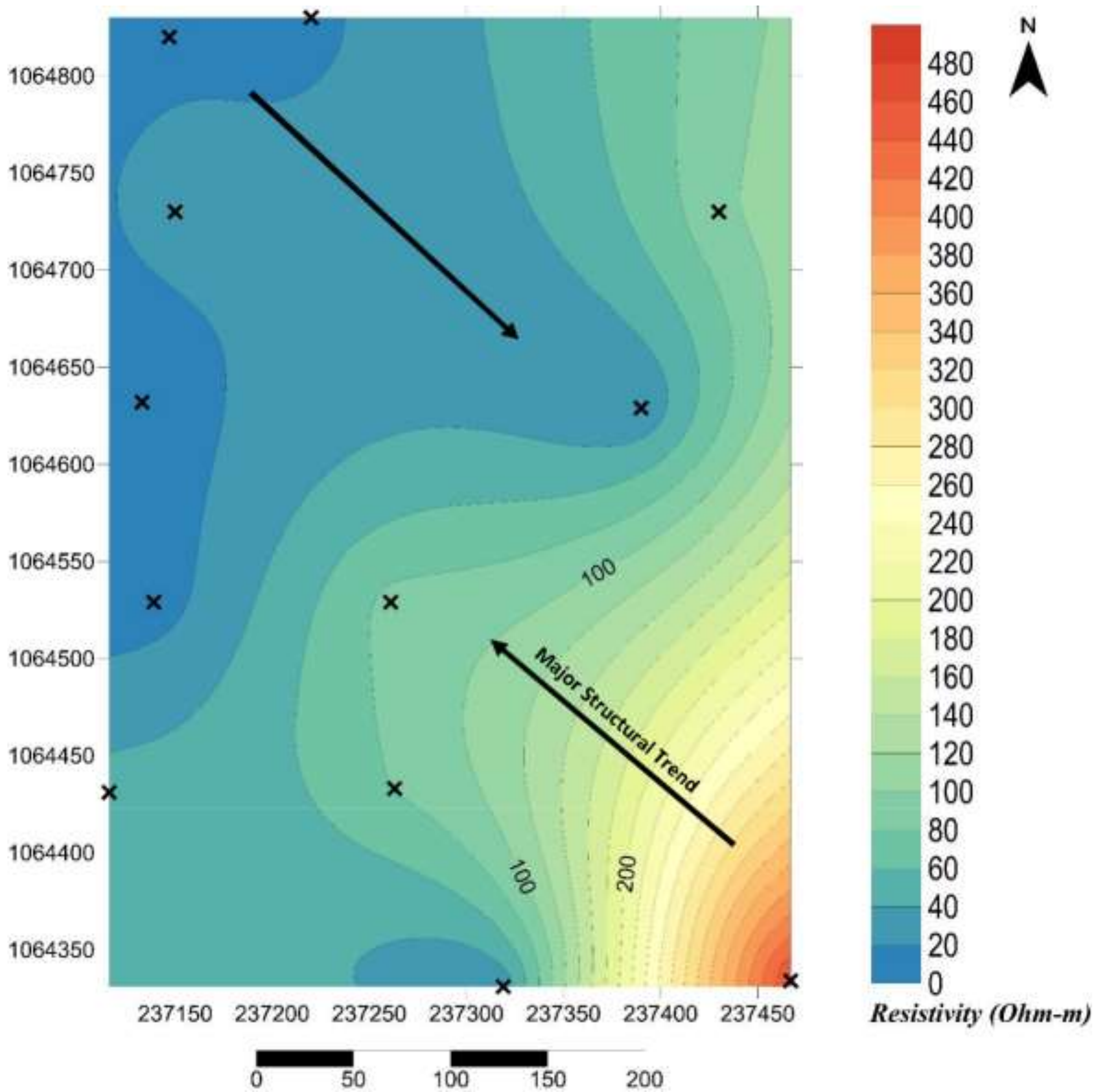

Figure 4.27: Generalised VES resistivity map of layer 2

Figure 4.28, is the generalised VES resistivity map of the third layer, inferred to chiefly constitute the basement of the entire study area, with varying degrees of resistivities spanning from 0 – 4000 Ωm.

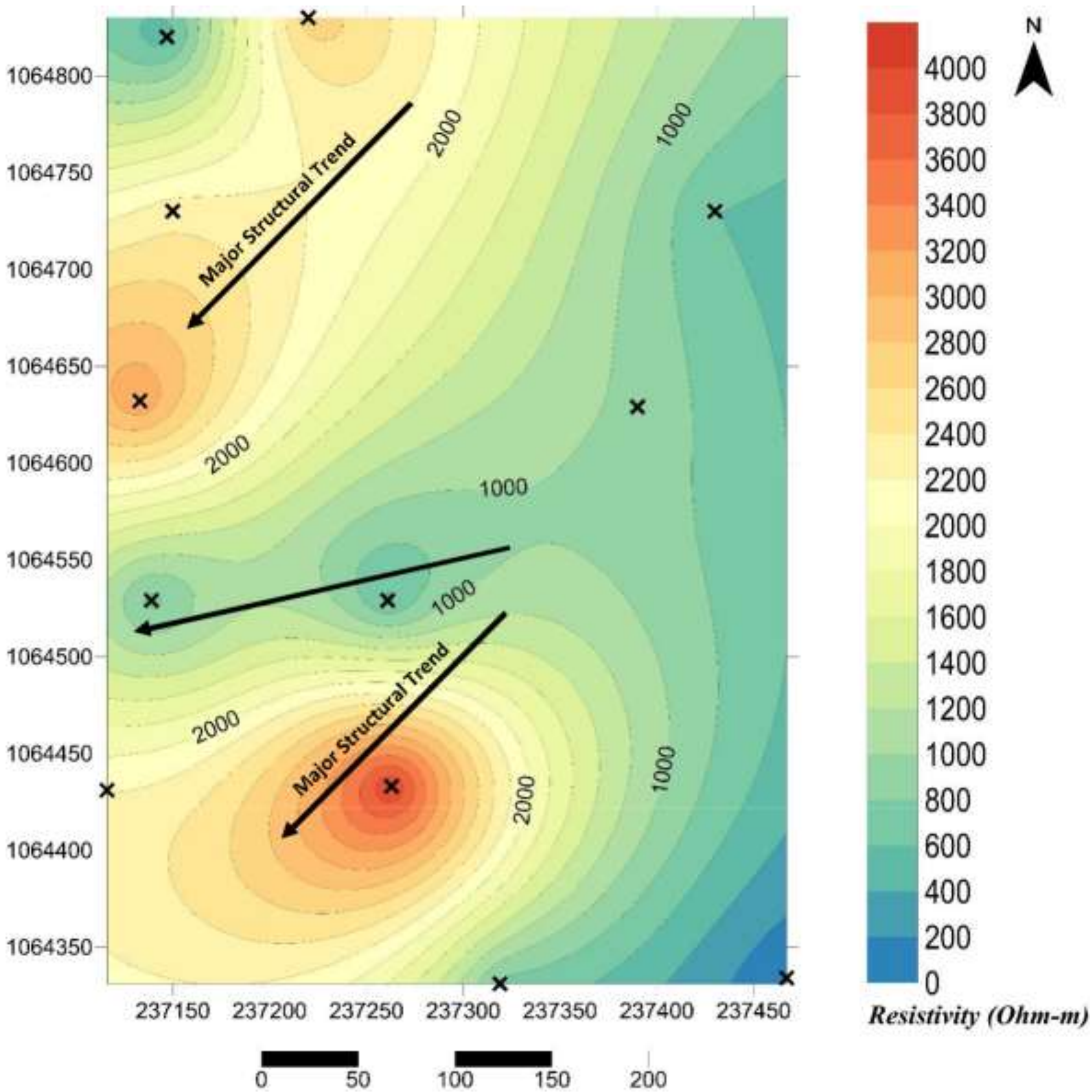

Figure 4.28: Generalised VES resistivity map of layer 3

Table 4.1 gives the summary of the VES sounding curves and the inferred possible mineral/rocks as compared with Table 3.

Table 4.1: Summary of sounding curve

VES	Layers	Resistivity (Ohm.m)	Depth (m)	Thickness (m)	Possible Minerals/Rocks	Curve Type
1	1	23.3	1.8	1.8	Sandstone, Clay,	H
	2	15.8	6.1	4.3	Schist,	
	3	2740.7	**	**	Magnetite ore, Granite	
2	1	28.0	1.4	1.4	Sandstone, Clay,	H
	2	18.0	5.5	4.1	Schist, Quartzite,	
	3	464.1	**	**	Granite	
3	1	70.6	0.9	0.9	Quartzites,	H
	2	26.6	12.8	11.9	Clayey Minerals	
	3	2309.3	**	**	Granite	
4	1	20.0	1.0	1.0	Saturated Sandstone,	H
	2	10.1	5.9	4.9	Clayey minerals, Schist	
	3	3195.5			Granodiorite	
5	1	14.4	2.3	2.3	Sandstone,	H
	2	10.1	9.9	7.6	Clayey Minerals,	
	3	713.0	**	**	Granodiorite	
6	1	66.7	0.8	0.8	Schist, Clay,	H
	2	23.8	15.2	14.4	Weathered granite,	
	3	1470.3	**	**	Granite	
7	1	15.9	0.9	0.9	Sandstone,	H
	2	464.3	11.4	10.6	Schist,	
	3	1523.3	**	**	Granodiorite	
8	1	18.6	3.2	3.2	Sandstone, Quartzite,	A
	2	113.2	6.6	3.4	Weathered granite	
	3	3195.2	**	**	Granitic rock	
9	1	71.6	0.9	0.9	Sandstone, Quartzite,	A
	2	86.3	6.5	5.6	Schist,	
	3	566.6	**	**	Weathered-fresh basement	
10	1	10.2	5.7	5.7	Clay, Sandstone,	H
	2	47.7	9.9	4.3	Schist,	
	3	2196.8	**	**	Granite	
11	1	78.1	1.0	1.0	Sandstone	HK
	2	21.7	4.6	3.6	Clayey Minerals, Quartzite	
	3	944.9	24.1	19.5	Granodiorite,	
	4	218.5	61.6	37.4	Weathered granite,	
	5	102.3	**	**	Saturated Sandstone	
12	1	154.6	1.0	1.0	Sandstone, Clay	H
	2	97.5	8.6	7.6	Schist,	
	3	534.0	**	**	Granodiorite	

CHAPTER FIVE

5.0 CONCLUSION AND RECOMMENDATIONS

5.1 Conclusion

The generalised conductivity map of the area shows a general conductive trend of NE-SW corresponding to the major structural trend in Nigeria. Significant conductivity responses due to inferred fracturing units containing conductive minerals as indicated by the peak responses of the current distributions in the six VLF profiles and the geologic features in the investigated areas of high conductivity were observed in all the six (6) profiles corresponding to fracture zones of interest as indicated in the current density sections, with profile 5 having the highest conductivity response of 135.5 mS/m and profile 6 with the least conductivity response of -136.7 mS/m.

The Vertical Electrical Soundings (VES) corresponding to significantly high and low VLF responses delineated lithological variations in the subsurface with possible areas of highly fractured/mineralised zones at average depth to conductive bodies at 9.2 m. A general H-type curve were observed at VES 01, 02, 03, 04, 05, 06, 07, 10 and 12, VES 08 and 09 gave rise to an A-type curve indicative of majorly basement rock of granitic nature, however, VES 11 had a HK-type curve with five major layers with possible presence of conductive and non-conductive minerals.

Hence, zones of high conductivity on the VLF profiles and corresponding VES points are susceptible to fractures/mineralisation which aligns to the findings by Ogungbemi *et al*. (2014), that mineralisation majorly occurs with fractured and zones of intrusions.

Based on the integration of geophysical and geological data available, the study area constitutes and exhibits possible features of conductive and non-conductive minerals, and the applied methods has proven great success in delineating the presence of near surface conductive mineral deposits.

5.2 Recommendations

Hence it is recommended that the results and findings be applied in conductive/solid mineral exploration in this area to verify its originality. It is also vital to employ a wide variety of geological field mapping and geochemical techniques to augment areas of geological lapses for professional mineral exploration and development.

5.3 REFERENCES

Adejuwon, B. B, Salami, A.A., Omotola, P.S., Ashien, S.O., Adeyemo, B.K., & Ujubuonu E.G. (2018). Integrated EM (VLF) gravity survey for delinetion of mineralized viens in Touzuwa Area of Benue State, Nigeria. *International Journal of Engineering Reseach and Technology, 7*(02), 49-53.

Adekoya, J.A., Kehinde, P. O.O., and Odukoya, A.M. (2011). Geological distribution of resources in Southwestern Nigeria. (M. O. Eduvie, Ed.) *Journal of MIning and Geology, 47*(1), 1-13.

Ajibade, A.C, Fitches, W.R, & Wright, J.B. (1979). The Zungeru mylonites, Nigeria: recognition of a major tectonic unit. *Rev. De Geol. Phys. 21,*, 359-363.

Ajibade, A.C., & Wright, J.B. (1989). The Togo-Benin-Nigeria shield: evidence of crustal aggregation in the Pan-African belt. *Tectonophysics, 165*, 125-129.

Akinlalu, A.A., Adelusi, A.O., Olayanju, G.M. Adiat, K.A.N., Omosuyi, G.O., Anifowose, A.Y.B., & Akeredolu, B.E. (2018). Aeromagnetic mapping of basement structures and mineralization characterization of Ilesa schist belt, Southwestern, Nigeria. *Journal of African Earth Sciences, 138,* 383-391.

Akintayo, O. O, Toyin, O. O & Olorunyomi J. A. (2014). Determination of the location and depth of mineral rocks of Olode Village in Ibadan, Oyo State, Nigeria, using geophysical methods. *International Journal of Geophysics*, 1-13.

Alan, E. M & Aftab, K. (2000). *Looking into the Earth: An Intoduction to Geological Geophysics.* New York: Cambridge University Press.

Alisa, A. M. (1990). *A Dictionary of Earth Science Ed.; "Telluric Current".* Oxford: University Press.

Arinze, J. I, Emedo, O. C, & Nwaga, A. C. (2018). Analysis of aeromagnetic anomalies and structural lineaments for mineral and hydrocarbon exploration in Ikom and its environs, Southeastern, Nigeria. *Journal of African Eartth Science, 151*, 274-285.

Austin, C. O, Chukwudi, C. E. (2014). A ground integrated geophysical exploration for sulfide ore deposits. case study: EPL A40 mine field, lower Benue trough, Nigeria. *Internationals Research Journl of Geology and Mining (IRJGM), 2*(8), 214-221.

Barley, M.E., Eisenlohr, B., Groves, D.I., Perring, C.S., & Vearncombe, I.R. (1989). Late Archean convergent margin tectonics and gold mineralisation. A new look at the Norsema-Wiluma belt, western Australia. *Geology 17,* 826-829.

Black, R. (1980). *Precambrian of West Africa* (Vol. 4).

Dogara, M.D, & Aloa, J.O. (2017). Preliminary estimate of gypsum deposit based on Wenner and Schlumberger electrical resistivity methds at Ikpeshi, Edo State, Nigeria. *Science World Journal*, 19-23.

Ejepu, J. S, Arikawe, E. A, Abdullahi, S. (2018). Geological multispectral and aeromagnetic expressions of pegmatite. *American Journal of Modern Physics and Application*, *5*(4), 53-69.

Elueze, A. (1981). Petrograhic studies of metabasic rocks and meta-ultramafites in relateion to mineralization in Nigerian schist belts. *J Mining Geol*, 18:31-36.

Evans, A. M. (1997). Environmental Geology. In A. M. Evans, *An Introduction to Economic Geology and Its Environmental Impact* (pp. 373-375). Oxford: Blockwell.

Evans, A. M. (2009). *Ore Geology and Industrial Minerals: An Introduction* (3 ed.). London: John Wiley & Sons.

Ezeh, C.L., Mamah, L.I, & Israel-Cookey, C. (2004). Very low frequency electromagnetic (VLF-EM) response from a lead sulphide lode in the Abakaliki lead/zinc field, Nigeria. *International Journal of Applied Earth Observation and Geo-Information*, *5*(2), 159-163.

Fraser, D. (1969). *Conrtouring of VLF-EM Data: Geophysics* (Vol. 34). New York.

GAMERS. (2018, August 11). *Map of Niger State, Nigeria*. Retrieved September 9, 2019, from Geospatial Analysis Mapping and Environmental Research Solutions: https://www.gamers.com.ng/map-of-niger-state-nigeria/

Gordon, R. (2016). *The Rebirth of VLF Geophysical Technology*. Retrieved February 25, 2019, from GEM System: www.eoas.ubc.ca

Jeng, Y., Lin, M.J. & Chen, C.S. (2004). *A very low frequency-electromagnetic study of the geo-enviromental hazardous areas in Taiwan.* Taiwan: Environ. Geol., 46.

Jones, F. (2007). *Geophysics foundation: Quick review: Summary of VLF surveying and data*. Retrieved June 16, 2019, from www.eoas.ubc.ca: www.eoas.ubc.ca/ubcgif/iag/foundations/method-summ_files/vlf-notes.htmm

Kearey, P. & Brooks, M. (1984). *An introduction to geophysical exploration.* Oxford: Blackwell.

Kearey, P., Brooks, M. & Hill, I. (2002). In K. P., *An introduction to geophysical exploration* (pp. 280-281). Oxfrod: Blockwell.

Keller G.V. & Frischknecht F.C. (1966). *Electrical methods in geophysical prospecting.* Oxford, New York, Toronto, Sydney, Braunschweig: Pergamon Press.

Kullenberg, L. (2015, SEPTEMBER 22). *Launch of the Airborne Geophysical Data.* Retrieved from THE WORLD BANK IBRD-IDA: https://www.worldbank.org/en/news/speech/2015/08/20/launch-of-the-airborne-geophysical-data

Lowrie, W. (2007). *Fundaamentals of Geophysics.* New York: CAMBRIDGE UNIVERSITY PRESS.

Marescot, L. (2004). Electrical Surveying. In L. Marescot, *Resistivity Method* (pp. 18-42). Zurich: Swiss Federal Istitute of Technology.

McGaughey, W.J., & Vallee, M.A. (1997). Ore Delineation in Three Dimension. *Proceedings of Exploration 97: Decennial International Conference on Mineral Exploration* (pp. 639-650). Canada: Noranda Technology Centre.

Mwenifunbo, C. (1997). Electrical Methods for Ore Body Delineation (Mine Site Exploration and Ore Delineation). (A. Gubins, Ed.) *Geological Survey of Canada*, 667-676.

Obaje, N. G. (2009). *Geology and Mineral Resources of Nigeria* (Vol. 772). (B. S. Bhattacharji, Ed.) Berlin: Springer.

Ogungbemi, O.S, Alu, O.O, & Ologe, O.O. (2014). Integrated geophysical approach to solid mineral exploration: a case study of Kusa mountain, Ijero Ekiti, Southwestern Nigeria. *Pacific Journal of Science and Technology, 15*(1), 426-432.

Olawuyi, A.K., Ako, B.D., Omosuyi, G.O. & Adelusi, A.O. (2016). Application of 3D euler deconvolution of aeromagnetic data and pseudo-gravity transforms in mineral exploration: a case study of the pegmatite rich zones of Lafiagi, Central Nigeria. *Arabian Journal of Geosciences*, 674.

Oluwaseun, I. G. (2013). *Mineral Prospecting and Exploration (with special references to Nigeria).* Ibadan: Disaster and Risk Management, Department of Geography, University of Ibadan.

Onwuegbuchulam, C.O., Ikoro, D.O., Nwugha, V.N., & Okereke, C.N. (2016). Application of very low frequency-electromagnetic (VLF-EM) method to monitor fracture/conductive zones in Auchi South-western Nigeria. *The International Journal of Engineering and Science, 5*(5), 7-13.

Osinowo, O. O, & Falufosi, M. O. (2018). Magnetic and very Llow frequency electromagnetic (VLF-EM) investigation for gold exploration around Ihale in Bunnu-Kabba Area of Kogi, North-Central Nigeria. *Contribution to Geophysics and Geodesy, 48*, 191-205. doi:10.2478/congeo-2018-0008

Pirttijärvi, M. (2004, February 20). Karous-Hjelt and Fraser filtering of VLF measurements. Oulu, Oulu, Finland.

Prasad, U. (2012). Economic Geology. In U. Prasad, *Economic Geology* (pp. 318-319). New Delhi: CBS.

Reynolds, J. M. (2011). *An Introduction to Applied and Environmental Geophysics* (2nd ed.). UK, West Sussex, Great Britain: Wiley-Blackwell.

Richard, C. B, Lynn, Y & Ronald D. K. (2013). Some Considerations for Selection and Successful Applicatio of Surface Geophysical methods. Tarrace, Maimi, USA.

Scott, W. (2014). *Geophysics for Mineral Exploration.* Canada: Newfoundland and Labrador. Retrieved from www

Shehu, S. J, Musa, O. A, Muhammad, S, Abdulrahim, A. B & Salihu, B. (2019). A reconnaisance study to delineate the potential mineral zones around the schist belt areas of Kano State, Nigeria using airborne magnetic Data. *Journal of Geology and Mining Research*, *11*(2), 14-21.

Sriramulu, G., Ramadass, G, & Dubba, V. K. (2017). Very low frequency, magnetic and radiometric surveys for lamporite investigation in Vattikod area of Nalgonda district, Telangana State, India. *Pelagia Research Library*, 138-145.

Talaat, M. R, Mohammed F. & Abdel F. (2010). Characterisation of gold mineralisation in Garin Hawal Area, Kebbi State, NW Nigeria, using remote sensing. *The Egyptian Journal of Remote Sensing and Space Science*, *13*(2), 153-163.

Telford, W. M., Geldart, L. P., & Sheriff, R. E. (1990). Applied Geophysics, Second Edition. In W. M. Telford, *Applied eophysics, Second Edition* (pp. 283-290). New York: Cambridge University Press.

Telford, W.M., Geldart, L.P., & Sheriff, R.E. (2001). *Applied Geophysics.* New York: Cambridge University Press.

Tijani, M. N., Osinowo, O. O , & Ogedenbe, O. (2009). Mapping of sub-surface fracture systems using integrated electrical resistivity profiling and VLF-EM methods: a case study of suspected gold mineralisation. *RMZ - Materials and Geo-environment, 56*(4), 415-436.

Usman, A. O, Chukwudi, C. E, Aurelius, O. O, & Augutine, I. C. (2019). Integration of aeromagnetic interpretation and induced polarization methods in delineating mineral deposits and basement configuration within Southern Bida Basin, North-West Nigeria. *Proceedings of the 1st Springer Conference of the Arabian Journal of Geosciences (CAJG-1)* (pp. 69-71). Tunisia: Springer.